

MATHEMATICAL MODELING OF LIQUID-FEED DIRECT METHANOL FUEL CELLS

A DISSERTATION

*Submitted in partial fulfilment of the
requirements for the award of the degree*

of

MASTER OF TECHNOLOGY

in

CHEMICAL ENGINEERING

(With Specialization in Computer Aided Process Plant Design)

By

PRIYANKA JAIN



DEPARTMENT OF CHEMICAL ENGINEERING
INDIAN INSTITUTE OF TECHNOLOGY ROORKEE
ROORKEE-247 667 (INDIA)

JUNE, 2005

CANDIDATE'S DECLARATION

I hereby declare that the work which is being presented in this dissertation entitled "**Mathematical Modeling of Liquid-Feed Direct Methanol Fuel Cells**", in partial fulfillment of the requirements for the award of the degree of **Master of Technology in Chemical Engineering** with specialization in **Computer Aided Process Plant Design**, submitted in the Department of Chemical Engineering, Indian Institute of Technology, Roorkee, India is an authentic record of my own work carried out during the period from September 2004 to May 2005, under the supervision and valued guidance of **Dr. S. C. Gupta**, Professor and **Dr. V. K. Agarwal**, Associate Professor, of Department of Chemical Engineering, Indian Institute of Technology, Roorkee, India.

The matter embodied in this dissertation has not been submitted by me for the award of any other degree or diploma.

Place: Roorkee, India.

Date: 30/06/2005


(Priyanka Jain)

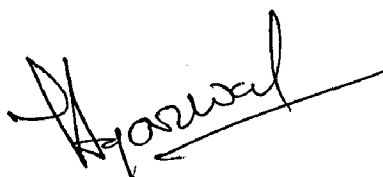
CERTIFICATE

This is certified that the above statement made by the candidate is correct to the best of our knowledge.



(Dr. S. C. Gupta)

Professor
Department of Chemical Engineering
Indian Institute of Technology
Roorkee, India.



(Dr. V. K. Agarwal)

Associate Professor
Department of Chemical Engineering
Indian Institute of Technology
Roorkee, India.

ACKNOWLEDGEMENTS

These few lines of acknowledgement can never substitute the deep appreciation that I have for all those without whose help, support and inspiration this dissertation would not have taken its present character.

I am deeply indebted to my guides **Dr. S. C. Gupta**, Professor and **Dr. V. K. Agarwal**, Associate Professor, Department of Chemical Engineering, Indian Institute of Technology, Roorkee, India, without whom the insight to initiate a work on mathematical modeling of liquid-feed direct methanol fuel cell would not have engrossed my deep interest. I would like to sincerely acknowledge their ardent supervision and valued guidance, relentless support, discerning thoughts and loads of inspiration that led me forward to delve deeper into the topic.

I am equally thankful to **Dr. B. Mohanty**, Head, Department of Chemical Engineering, Indian Institute of Technology, Roorkee, India, for his constant invigoration at each stage which enthused my work spirits.

I do not have words to thank **Dr. I. M. Mishra**, Chairman D.R.C, Department of Chemical Engineering, Indian Institute of Technology, Roorkee, India, for his valued guidance and kind cooperation to make this work a success.

I express my gratitude to the personnel at CAD Lab, Department of Chemical Engineering, Indian Institute of Technology, Roorkee, India, for their assistance, cooperation and in making available the computing facility as and when required during the course of the work.

Above all, my faith and the blessings of God have always provided the required psychological and spiritual support to stay strong and dedicated even in the most demanding situations. My parents, though not present anymore in physical form; deserves the utmost acknowledgement for cultivating in me the system of values and instincts that shall always enlighten my path, as well inspire me in my future endeavors.

Priyanka Jain
(PRIYANKA JAIN)

Abstract

The present investigation pertains to a theoretical study of simulation of liquid-feed direct methanol fuel cell. Basically it deals with the development of mathematical model for analysis of thermo- and electrochemical properties of the liquid-feed direct methanol fuel cell. It also includes the algorithm for the mathematical solution of the model. Further, the comparison of the proposed model has been done with a reference model as suggested by *Z. H. Wang* and *C. Y. Wang*¹. The polarization curves of DMFC obtained through the model has been considered as the basis of comparison. Finally, studies of the effect of different operating variables viz. temperature, pressure and fuel flow rate has been done.

Using the basic principle of thermodynamics and electrochemistry a mathematical model of liquid-feed direct methanol fuel cell under ideal gas condition has been developed. The underline equations include calculation of component partial pressures, Gibbs free energy, change in enthalpy and EMF. An algorithm has been developed for solution of the model.

The model developed is compared and validated against the reference model as proposed by *Z. H. Wang* and *C. Y. Wang*¹. An examination of the fuel cell *polarization curve* obtained by solving the model show that the model has been successful in representing the liquid-feed direct methanol fuel cell and has been found to be in agreement with the polarization curve as obtained by the reference model. The maximum deviation between the profiles obtained by this simulation and of *Z. H. Wang* and *C. Y. Wang*¹ was found to be 10%.

CONTENTS

	Page No.
CANDIDATE'S DECLARATION	i
ACKNOWLEDGEMENT	ii
ABSTRACT	iii
LIST OF FIGURES	iv
LIST OF TABLES	v
Chapter 1 : INTRODUCTION	1
1.1 WHAT IS FUEL CELL	1
1.1.1 Fuel Cell Description	2
1.1.2 Fuel Cell Types	3
1.1.3 Fuel Cell Characteristics	4
1.2 OBJECTIVE OF THESIS	5
1.3 ORGANIZATION OF THESIS	5
Chapter 2 : LITERATURE SURVEY	7
2.1 GENERAL	7
2.2 OPERATING PRINCIPLE OF DMFC	11
2.3 CHEMICAL THERMODYNAMICS	12
2.3.1 Criterion for Spontaneous Reaction	14
2.3.2 Effect of Temperature and Pressure on ΔG	15
2.3.3 Equilibrium of Gas Mixture	16
2.3.4 Nernst Equation	17
2.4 WORKING OF DMFC	18
2.4.1 DMFC Process	21
2.4.2 Byproducts of DMFC	22

2.4.3	Advantages of DMFC over other Fuel Cells	23
Chapter 3 :	MATHEMATICAL ANALYSIS AND MODELING	24
3.1	MODEL DEVELOPMENT	24
3.1.1	Calculation Stages	25
Chapter 4 :	SOLUTION OF MODEL	31
4.1	SOLUTION OF THERMODYNAMIC EQUATIONS	31
Chapter 5 :	RESULTS AND DISCUSSION	36
5.1	VALIDITY OF MODEL	37
5.2	EFFECT OF VARIABLES	38
5.2.1	Effect of Temperature	39
5.2.2	Effect of Pressure	39
5.2.3	Effect of Fuel Flow Rate	39
Chapter 6 :	CONCLUSION AND RECOMMENDATIONS	47
6.1	CONCLUSION	47
6.2	RECOMMENDATIONS	47
	REFERENCES	49
	ANNEXURE – A	53
	ANNEXURE – B	54
	ANNEXURE – C	58
	NOMENCLATURE	62

LIST OF TABLES

Table No.	Title	Page No.
Table 5.1	Range of operating parameters	36
Table 5.2	Model validation	38
Table A.1	Std. Gibbs free energy of formation	46
Table A.2	Change in enthalpy of formation	46
Table A.3	Heat capacity coefficients	46
Table C.1	Calculated data: Gibbs free energy	51
Table C.2	Calculated data: change of enthalpy	51
Table C.3	Calculated data: net work output	52
Table C.4	Calculated data: thermal efficiency	52
Table C.5	Calculated data: Nernst potential	53
Table C.6	Calculated data: cell current	53
Table C.7	Calculated data: current density	54
Table C.8	Calculated data: cell voltage	54

LIST OF FIGURES

Fig. No.	Title	Page No.
Fig 2.1	Basic DMFC operation	7
Fig. 2.2	Schematic of a DMFC	12
Fig. 2.3	Design of a DLFC module	19
Fig. 2.4	Reaction scheme and principle of a DMFC	19
Fig. 2.5 (a)	Functioning of DMFC	20
Fig. 2.5 (b)	Functioning of DMFC	20
Fig. 2.6	Schematic of operating principle of DMFC	22
Fig. 4.1	Algorithm for the solution of mathematical model	22
Fig. 5.1	Variation in Gibbs free energy with Temp. & Pressure	40
Fig. 5.2	Variation in change of enthalpy with temperature	41
Fig. 5.3	Variation in thermal efficiency with temperature	42
Fig. 5.4	Variation in net work output with temperature	43
Fig. 5.5	Variation in Nernst potential with temperature	44
Fig. 5.6	Variation in cell current with fuel flow rate	45
Fig. 5.7	Variation in cell voltage with current density	46

Introduction

Poor energy use is a problem that runs rampant throughout developing economies and must be solved before these economies can truly progress. Many factors contribute towards poor energy usage, including inefficient or insecure power generation and transmission capabilities, inefficient industrial and manufacturing processes, lack of sufficient infrastructure, and lack of reliable and clean fuel sources. These factors not only affect the economies of the developing countries, but the health and quality of life of the countries' inhabitants. Two billion people in the world have no access to electricity. Those of us who do have access to electricity are finding its availability to be increasingly expensive, a pollution threat, and diminishing in supply. One billion, energy-using people have created the environmental problems we have today. What will the world be like when the other billions of people begin using energy like we do?

Fuel cells – clean and efficient distributed power technologies can help provide a solution and are an up-and-coming answer to this energy debate, and may increase in popularity as the governments move toward the deregulation of the utility industry. Despite their modern high-tech aura, fuel cells actually have been known to science for more than 150 years. Though generally considered a curiosity in the 1800s, fuel cells have become the subject of intense research and development, especially since World War II.

1.1 What Is a Fuel Cell?

As early as 1839, William Grove discovered the basic operating principle of fuel cells by reversing water electrolysis to generate electricity from hydrogen and oxygen. The principle that he discovered remains unchanged today.

A fuel cell is an electrochemical “device” that continuously converts chemical energy into electric energy (and some heat) for as long as fuel and oxidant are supplied.

Fuel cells therefore bear similarities both to batteries, with which they share the electrochemical nature of the power generation process, and to engines, which — unlike batteries — will work continuously consuming a fuel of some sort. Here is where the analogies stop, though. Unlike engines or batteries, a fuel cell does not need recharging, it

operates quietly and efficiently, and — when hydrogen is used as fuel — it generates only power and drinking water. Thus, it is a so-called *zero emission engine*. Thermodynamically, the most striking difference is that thermal engines are limited by the *Carnot efficiency* while fuel cells are not.

Grove's fuel cell was a fragile apparatus filled with dilute sulfuric acid into which platinum electrodes were dipped. From there to modern fuel cell technology has been an exciting but long and tortuous path.

1.1.1 Fuel Cell Description

Fuel cells are electrochemical devices that convert the chemical energy of a reaction directly into electrical energy. The basic physical structure, or building block, of a fuel cell consists of an electrolyte layer in contact with a porous anode and cathode on either side. In a typical fuel cell, gaseous fuels are fed continuously to the anode (negative electrode) and an oxidant (i.e., oxygen from air) is fed continuously to the cathode (positive electrode); the electrochemical reactions take place at the electrodes to produce an electric current. The fuel or oxidant gases flow past the surface of the anode or cathode opposite the electrolyte and generate electrical energy by the electrochemical oxidation of fuel, and the electrochemical reduction of the oxidant, usually oxygen. In theory, any substance capable of chemical oxidation that can be supplied continuously (as a fluid) can be burned galvanically as fuel at the anode of a fuel cell. Similarly, the oxidant can be any fluid that can be reduced at a sufficient rate. A three-phase interface is established among the reactants, electrolyte, and catalyst in the region of the porous electrode. The nature of this interface plays a critical role in the electrochemical performance of a fuel cell, particularly in those fuel cells with liquid electrolytes. In such fuel cells, the reactant gases diffuse through a thin electrolyte film that wets portions of the porous electrode and react electrochemically on their respective electrode surface. If the porous electrode contains an excessive amount of electrolyte, the electrode may "flood" and restrict the transport of gaseous species in the electrolyte phase to the reaction sites. The consequence is a reduction in the electrochemical performance of the porous electrode. Thus, a delicate balance must be maintained among the electrode,

electrolyte, and gaseous phases in the porous electrode structure. Much of the recent effort in development of fuel cell technology has been devoted to reducing the thickness of cell components while refining and improving the electrode structure and the electrolyte phase, with the aim of obtaining a higher and more stable electrochemical performance while lowering cost. The electrolyte not only transports dissolved reactants to the electrode, but also conducts ionic charge between the electrodes and thereby completes the cell electric circuit. It also provides a physical barrier to prevent the fuel and oxidant gas streams from directly mixing.

The functions of porous electrodes in fuel cells are: 1) to provide a surface site where gas/liquid ionization or de-ionization reactions can take place, 2) to conduct ions away from or into the three phase interface once they are formed (so an electrode must be made of materials that have good electrical conductance), and 3) to provide a physical barrier that separates the bulk gas phase and the electrolyte. A corollary of Item 1 is that, in order to increase the rates of reactions, the electrode material should be catalytic as well as conductive, porous rather than solid. The catalytic function of electrodes is more important in lower temperature fuel cells and less so in high temperature fuel cells because ionization reaction rates increase with temperature. It is also a corollary that the porous electrodes must be permeable to both electrolyte and gases, but not such that the media can be easily "flooded" by the electrolyte or "dried" by the gases in a one-sided manner.

1.1.2 Fuel Cell Types

A variety of fuel cells are in different stages of development. They can be classified by use of diverse categories, depending on the combination of type of fuel and oxidant, whether the fuel is processed outside (external reforming) or inside (internal reforming) the fuel cell, the type of electrolyte, the temperature of operation, whether the reactants are fed to the cell by internal or external manifolds, etc. The most common classification of fuel cells is by the type of electrolyte used in the cells and includes 1) *polymer electrolyte fuel cell (PEFC)*, 2) *alkaline fuel cell (AFC)*, 3) *phosphoric acid fuel cell (PAFC)*, 4) *molten carbonate fuel cell (MCFC)*, and 5) *solid oxide fuel cell (SOFC)*. These fuel cells are listed in the order of approximate operating temperature, ranging

from ~ 80 °C for PEFC, ~ 100 °C for AFC, ~ 200 °C for PAFC, ~ 650 °C for MCFC, ~ 600 - 1000 °C for SOFC. The operating temperature and useful life of a fuel cell dictate the physico-chemical and thermo-mechanical properties of materials used in the cell components (i.e., electrodes, electrolyte, interconnect, current collector, etc.). Aqueous electrolytes are limited to temperatures of about 200 °C or lower because of their high water vapor pressure and rapid degradation at higher temperatures. The operating temperature also plays an important role in dictating the type of fuel that can be used in a fuel cell. The low-temperature fuel cells with aqueous electrolytes are, in most practical applications, restricted to hydrogen as a fuel. In high temperature fuel cells, CO and even CH₄ can be used because of the inherently rapid electrode kinetics and the lesser need for high catalytic activity at high temperature.

1.1.3 Fuel Cell Characteristics

Fuel cells have many characteristics that make them favorable as energy conversion devices. Two that have been instrumental in driving the interest for terrestrial application of the technology are the combination of relatively high efficiency and very low environmental intrusion (virtually no acid gas or solid emissions). Efficiencies of present fuel cell plants are in the range of 40 to 55% based on the lower heating value (LHV) of the fuel. In addition, fuel cells operate at a constant temperature, and the heat from the electrochemical reaction is available for cogeneration applications. Because fuel cells operate at nearly constant efficiency, independent of size, small fuel cell plants operate nearly as efficiently as large ones. Thus, fuel cell power plants can be configured in a wide range of electrical output, ranging from watts to megawatts. Fuel cells are quiet and, even though fuel flexible, they are sensitive to certain fuel contaminants that must be minimized in the fuel gas.

The two major impediments to the widespread use of fuel cells are 1) high initial cost and 2) high-temperature cell endurance. These two aspects are the major focus of manufacturers' technological efforts.

Other characteristics that fuel cells and fuel cell plants offer are:

- Direct energy conversion (no combustion).
- No moving parts in the energy converter.
- Quiet.

- Demonstrated high availability of lower temperature units.
- Fuel flexibility.
- Demonstrated endurance/reliability of lower temperature units.
- Good performance at off-design load operation.
- Modular installations to match load and increase reliability.
- Remote/unattended operation.
- Size flexibility.
- Rapid load following capability.

General negative features of fuel cells include:

- Market entry cost high; N_{th} cost goals not demonstrated.
- Unfamiliar technology to the power industry.
- No infrastructure.

1.2 Objective of Thesis

- Mathematical analysis of a fuel cell
- To develop a mathematical model for the thermodynamic analysis of the fuel cell principles. Liquid-feed direct methanol fuel cell (DMFC) has been considered for this purpose. The main reasons for selecting the liquid-feed DMFC are:
 - Design characteristic: No need of a fuel vaporizer or ‘reformer’
 - Operating Characteristic: No need of high temperature or pressure
 - Applicability: Promising for applications in portable electronic devices.
- Solution of the mathematical model
- Comparison of the proposed model with that of *Z. H. Wang* and *C. Y. Wang*¹

1.3 Organization of Thesis

The thesis has been organized in six chapters. Chapter Two describes the thermodynamics of the some of the chemical reactions normally encountered in mathematical modeling of fuel cells and also the models available in literature are reviewed. Chapter Three presents the development of mathematical model. Fourth

Chapter presents the solution of the model and its results, discussion and validation have been given in Chapter Five. Finally Chapter Six highlights the main conclusions of the thesis and provides the recommendation for future work.

Literature Review

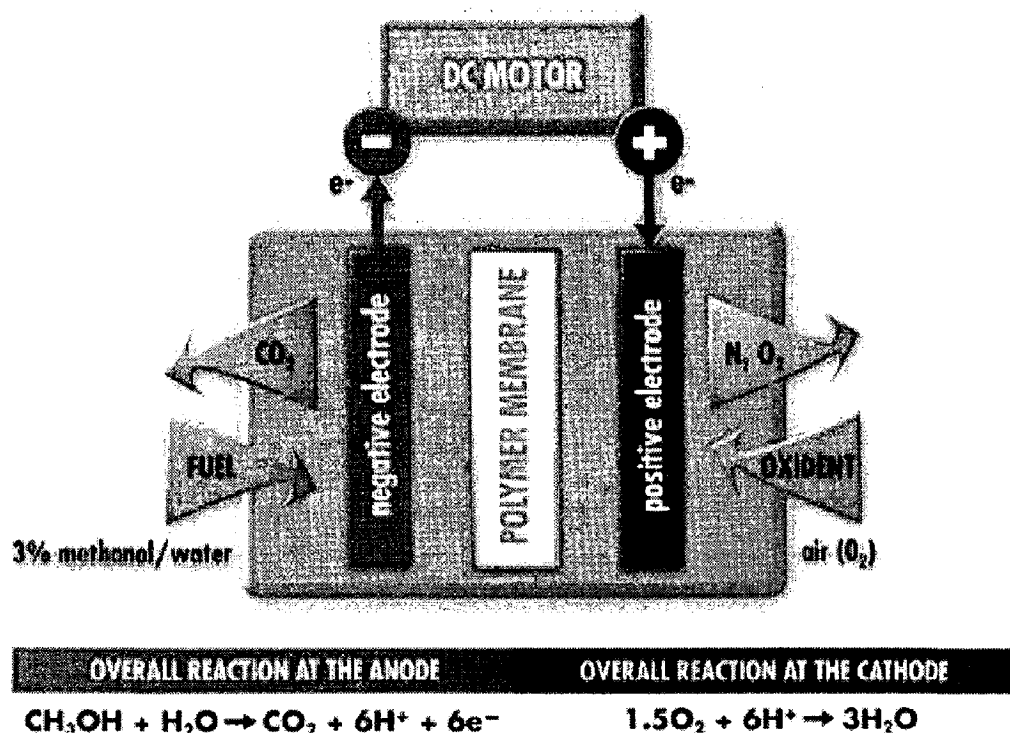


FIGURE 2.1 Basic Direct Methanol Fuel Cell Operation (Source: Methanol Institute)

No doubt one of the most elegant solutions to the fueling problem would be to make fuel cells operate on a liquid fuel. This is particularly so for transportation and the portable sector. The *direct methanol fuel cell* (DMFC), a liquid- or vapor-fed PEM fuel cell operating on a methanol/water mix and air, therefore deserves careful consideration. The main technological challenges are the formulation of better anode catalysts to lower the anode over potentials (currently several hundred milli-volts at practical current densities), and the improvement of membranes and cathode catalysts in order to overcome cathode poisoning and fuel losses by migration of methanol from anode to cathode.

The *direct methanol fuel cell* (DMFC) is often considered to be the ideal fuel cell system since it operates on a liquid fuel, which for transportation applications can potentially be distributed through the current petroleum distribution network. In addition, the DMFC power system is inherently simpler and more attractive than the conventional indirect methanol fuel cell, which relies on expensive and bulky catalytic reformer systems to convert methanol to hydrogen fuel. DMFC systems are potentially cost effective, but only

if they can meet the power requirement necessary for a commercially viable appliance. Unfortunately, commercialization of the DMFC has been slow because of its reduced performance compared to H₂/O₂ systems, amounting to traditionally no more than one quarter of the power densities, currently achieved with H₂ proton exchange membrane fuel cells (PEMFCs). The major limitation of the DMFC is the reduced performance of the anode, where more efficient *methanol electro-oxidation* catalysts are urgently needed. This limitation has prompted a large research effort to search for efficient methanol oxidation catalyst materials — yet it appears that only platinum-based materials show reasonable activity and the required stability. The availability of proton exchange membrane (PEM) materials has extended the operational temperature of DMFCs beyond those attainable with traditional *liquid electrolytes* and has led to major improvements in performance over the past ten years. More recently, the DMFC system has received more attention as the power densities of MEAs have improved. The performances of DMFCs are now in a range that seems feasible for small portable applications; as a consequence, this type of application has been identified as a niche market, which the DMFC could dominate because of reduced system complexity.

However, the wide application of DMFC is still hindered by several technological problems, low electro-activity of methanol oxidation on the anode, substantial methanol crossover through the polymer membrane, and severe cathode flooding. The cell performance is limited by anode kinetics due to its low exchange current density. Methanol crossover further causes lower open-circuit voltage (OCV) and waste of fuel and hence lower energy conversion efficiency. Water management greatly influences the cathode performance^{2, 3}.

Much work has been focused on the anodic oxidation of methanol.² The mechanism of the electro catalytic oxidation of methanol at the anode was postulated.^{3,4} Different anode catalyst structures of Pt-Ru were developed,⁵ and several anode catalysts other than Pt-Ru were explored.⁶⁻⁸ Additionally, the effects of the anode electrochemical reaction on cell performance were experimentally studied.⁹⁻¹¹

Methanol crossover in DMFC has been extensively studied both experimentally and theoretically. Narayanan *et al.*¹² and Ren *et al.*¹³ measured the methanol crossover flux with different membrane thicknesses and showed that the methanol crossover rate is inversely proportional to the membrane thickness at a given cell current density, thus indicating that diffusion is dominant. In addition, Ren *et al.*¹⁴ compared the diffusion with electro-osmotic drag processes and demonstrated the importance of the electro-osmotic drag in the methanol transport through the membrane. In their analysis, the methanol electro-osmotic drag is considered as a convection effect and the diluted methanol moves with electro-osmotically dragged water molecules. Tricoli *et al.*¹⁵ compared the methanol transport in two types of membranes. Valdez and Narayanan¹⁶ studied the temperature effects on methanol crossover and showed that the methanol crossover rate increases with cell temperature. Hikita *et al.*¹⁷ measured methanol crossover and cell performance under different membrane thickness and methanol feed concentrations. Their experiments showed that the cell performance during operation is affected by methanol crossover but not significantly dependent on methanol crossover flux in the case of sufficient oxygen supply. Ravikumar and Shukla¹¹ operated the liquid-feed DMFC at the oxygen pressure of 4 bars and found that the cell performance is greatly affected by methanol crossover at the methanol feed concentration greater than 2 M, and that this effect aggravates with the operating temperature. Wang *et al.*¹⁸ analyzed the chemical compositions of the cathode effluent of a DMFC with a mass spectrometer. They found that the methanol crossing over the membrane is completely oxidized to CO₂ at the cathode in the presence of a Pt catalyst. Additionally, the cathode potential is influenced by the mixed potential phenomenon due to simultaneous methanol oxidation and oxygen reduction as well as poisoning of Pt catalysts by methanol oxidation intermediates. Kauranen and Skou¹⁹ presented a semi-empirical model to describe the methanol oxidation and oxygen reduction reactions on the cathode and concluded that the oxygen reduction current is reduced in the presence of methanol oxidation due to surface poisoning.

In spite of these challenges, progress in the DMFC performance has been made steadily by many groups, *e.g.*, Halpert *et al.*²⁰ of Jet Propulsion Laboratory (JPL) and Giner, Inc.,

Baldauf and Preidel²¹ of Siemens, Ren *et al.*²² of Los Alamos National Laboratory (LANL), and Mench *et al.*,^{23,24} and Lim and Wang⁵¹ of the Penn State University. A comparative study of DMFC with hydrogen PEMFC was presented most recently by the LANL group.^{25, 26}

While attempts are continuing to elucidate the fundamental electrochemical reaction mechanisms, to explore new compositions and structures of catalysts, and to develop new membranes and methods for preventing methanol crossover, important system issues on DMFC are emerging, such as water management, gas management, flow field design and optimization, and cell up-scaling for different applications. A number of physicochemical phenomena take place in liquid-feed DMFC, including species, charge, and momentum transfer, multiple electrochemical reactions, and gas-liquid two-phase flow in both anode and cathode. Carbon dioxide evolution in the liquid-feed anode results in strongly two-phase flow, making the processes of reactant supply and product removal more complicated. All these processes are intimately coupled, resulting in a need to search for optimal cell design and operating conditions. A good understanding of these complex, interacting phenomena is thus essential and can be most likely achieved through a combined mathematical modeling and detailed experimental approach.

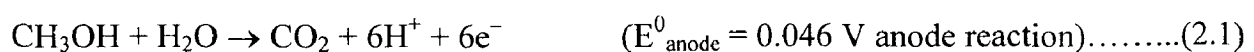
Baxter *et al.*²⁷ developed a one-dimensional mathematical model for a liquid-feed DMFC, mainly focused on the anode catalyst layer. A major assumption of their study was that the carbon dioxide is only dissolved in the liquid and hence their model of transport and electrochemical processes in the anode catalyst layer is single-phase only. Using a macro-homogeneous model to describe the reaction and transport in the catalyst layer of vapor-feed anode, Wang and Savinell²⁸ discussed the effects of the anode catalyst layer structure on cell performance. Kulikovsky *et al.*²⁹ simulated a vapor-feed DMFC with a two-dimensional model and compared the detailed current density distributions in backing, catalyst layer, and membrane separator between conventional and alternative current collectors. In another paper, Kulikovsky³⁰ numerically studied a liquidfeed DMFC considering methanol transport through the liquid phase and in hydrophilic pores of the anode backing. In both publications of Kulikovsky, the important phenomenon of

methanol crossover was ignored. Dohle *et al.*³¹ presented a one-dimensional model for the vapor-feed DMFC, and the crossover phenomenon was described. The effects of methanol concentration on the cell performance were studied. Scott *et al.*³²⁻³⁵ also developed several simplified single-phase models to study transport and electrochemical processes in liquid-feed DMFC and showed that the cell performance is limited by the slow diffusion of methanol in liquid.

In a recent paper, Wang & Wang³⁶, suggested a comprehensive model for two-phase flow, multi-component transport, and detailed electrochemical reactions are presented for a liquid-feed DMFC, including electrodes, channels, and PEM separator. The model was intended to provide a useful tool for the basic understanding of electrochemical phenomena in DMFC and for the optimization of cell design and operating conditions. The model was solved and validated against experimental performance data. The electrochemical processes were numerically analyzed and the effects of the anode feed methanol concentration on cell performance were studied in detail to illustrate the utility of the model. The effect of methanol crossover on cell performance was also explored.

2.2 Operating Principle of the DMFC

Methanol and water electrochemically react (i.e., methanol is electro-oxidized) at the anode to produce carbon dioxide, protons, and electrons as shown in Eq. (2.1). An acidic electrolyte is advantageous to aid CO₂ rejection since insoluble carbonates form in alkaline electrolytes. The protons produced at the anode migrate through the polymer electrolyte to the cathode where they react with oxygen (usually from air) to produce water as shown in Eq. (2.2). The electrons produced at the anode carry the free energy change of the chemical reaction and travel through the external circuit where they can be made to do useful work, such as powering an electric motor. A schematic of a DMFC is shown in Fig. 2.1.



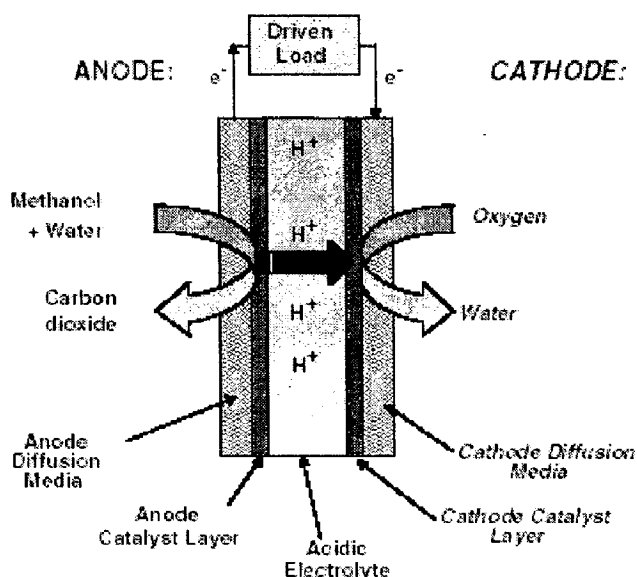
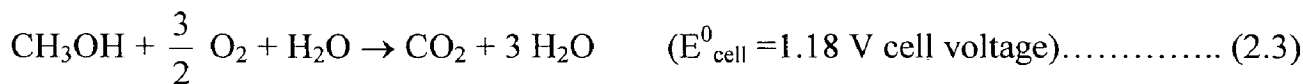
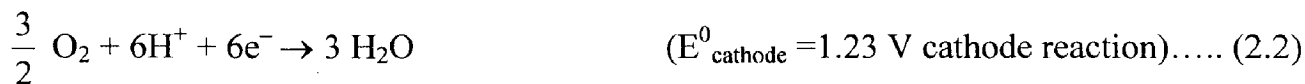


FIGURE 2.2 Schematic of a DMFC

2.3 Chemical Thermodynamics

Electrochemical cells such as fuel cells operate at constant temperatures with the products of the reaction leaving at the same temperature as the reactants. Because of this isothermal reaction, more of the chemical energy of the reactants is converted to electrical energy instead of being consumed to raise the temperature of the products; the electrochemical conversion process is therefore less irreversible than the combustion reaction. In the electrochemical cell, none of the criteria that define heat engines satisfied, so the Carnot cycle efficiency, which limits the maximum work to the highest temperature of the cycle, is irrelevant to electrochemical cells. Instead, the maximum work for an electrochemical cell, $W_{\text{max, cell}}$, is equal to the change in the Gibbs function (or Gibbs energy), ΔG , between products and reactants.

$$W_{\text{max, cell}} = -\Delta G \quad (2.4)$$

(The derivation is presented later in Section 3.4.4). The work, which is done by the movement of electrons through a difference in electrical potential, is denoted W_{cell} in Eq. (2.5). In electrical terms, the work done by electrons with the charge $n_e F$ moving through a potential difference, E is:

$$W_{\text{cell}} = n_e F E \quad (2.5)$$

In Eq. (2.5), n_e is the number of electrons transferred per mole of fuel and F is the charge carried by a mole of electrons, which is *Faraday's number* (96,485 C/mole⁻¹).

Chemical reactions proceed in the direction that minimizes the Gibb's energy. The change in Gibb's energy is negative as the reaction approaches equilibrium, and at chemical equilibrium the change in Gibb's energy is zero. The maximum work that an electrochemical cell can perform is equal to the change in the Gibb's energy as the reactants go to products. This work is done by the movement of electrical charge through a voltage, and at equilibrium the voltage is related to the change in Gibbs energy as shown earlier in Eq. (2.4). The Nernst equation is based on the Gibbs energy change and is derived in the later section.

The basis for the equations in this section is the definition of Gibb's energy.

$$G = H - TS \quad (2.6)$$

In the differential form, the Gibb's energy becomes

$$dG = dH - TdS - SdT$$

Substituting the definition of enthalpy for H gives

$$dG = d(U + PV) - TdS - SdT$$

$$dG = dU + PdV + VdP - TdS - SdT$$

The first term, dU , is replaced by the First Law of Thermodynamics to give the general expression for the change in Gibb's energy as applied to a *closed* (properties constant with time; $E = 0$), stationary system:

$$dG = \delta Q - \delta W + PdV + VdP - TdS - SdT \quad (2.7)$$

2.3.1 Criterion for a Spontaneous Reaction

The Gibb's energy is a function of temperature and pressure, and the effects of T and P on ΔG are shown in the following derivation based on Eq. (3.56). For a reversible process, δQ and TdS in Eq. (2.7) cancel because of the Second Law relationship. If the system is restricted to doing only expansion work, then δW and PdV cancel:

$$dG = \delta Q - \delta W + PdV - TdS$$

If the system is restricted to doing only expansion-type work, δW cancels with PdV to give Eq. (2.8).

$$dG = \delta Q - TdS \tag{2.8}$$

The Second Law of following equation:

$$dS = \left(\frac{\delta Q}{T} \right)_{rev}$$

is rewritten with an inequality sign ($=$ for a reversible and \geq for an irreversible process), and it is substituted into Eq. (2.8) to give Eq. (2.9).

$$dS \geq \left(\frac{\delta Q}{T} \right)_{rev,irrev} \tag{2.9}$$

$$\delta Q - TdS \leq 0$$

With the Second Law, Eq. (2.8) becomes

$$dG = \delta Q - TdS \leq 0$$

Therefore, in Eq. (2.10), to satisfy the Second Law, a reaction at constant temperature and pressure (T,P) will proceed in a direction of a negative change in Gibb's energy to the point where it reaches a minimum, $dG = 0$. When $dG = 0$, the reaction is at equilibrium.

$$(dG)_{T, P} \leq 0 \quad (2.10)$$

If the change is positive, the reaction violates the Second Law of Thermodynamics.

2.3.2 The Effect of Temperature and Pressure on ΔG

The Gibbs energy is a function of temperature and pressure, and the effects of T and P on ΔG are shown in the following derivation based on Eq. (2.7). For a reversible process, δQ and TdS in Eq. (2.7) cancel because of the Second Law relationship. If the system is restricted to doing only expansion work, then δW and PdV cancel:

$$dG = VdP - SdT \quad (2.11)$$

For an ideal gas, if T is constant, the Gibbs energy at one pressure can be determined with respect to its value at a reference pressure. The ideal gas equation of state begins the derivation for an expression that shows the pressure dependency of the Gibbs function:

$$PV = nRT$$

In the ideal gas equation, n is the number of moles, R is the molar gas constant, and T is the absolute temperature.

For an isothermal process, Eq. (2.11) becomes:

$$dG = VdP$$

The ideal gas equation is substituted for V ,

$$dG = nRT \frac{dP}{P}$$

and the differential is integrated.

$$\int_1^2 dG = nRT \int_1^2 \frac{dP}{P}$$

The Gibbs energy change for a change in pressure at constant temperature is

$$G_2 - G_1 = nRT \ln \left(\frac{P_2}{P_1} \right)$$

$$G_2 = G^0 + nRT \ln \left(\frac{P_2}{P_0} \right) \quad (2.12)$$

Eq. (3.61) can be rewritten in a molar quantity (lowercase) (kJ/mol) and denoted by the overhead bar, —:

$$\bar{g}_2 = \bar{g}^0 + nRT \ln \left(\frac{P_2}{P_0} \right)$$

The standard Gibb's energy at the reference state is a function only of temperature, and the pressure term allows the Gibb's to be calculated for different pressures. In thermodynamics texts, the standard Gibb's function is tabulated in terms of temperatures at a fixed reference pressure ($P^0 = 1 \text{ atm}$).

$$\bar{g}_1 (T, P_1) = \bar{g}_1^0 + nRT \ln \left(\frac{P_1}{P_0} \right) \quad (2.13)$$

2.3.3 Equilibrium of a Gas Mixture

For a chemical reaction occurring at constant temperature and pressure, the reactant gases A and B form products M and N. The stoichiometric coefficients are written with the italicized, lowercase letters *a*, *b*, *m*, and *n*.



The change in the Gibbs energy, ΔG , is denoted as the difference between the products and reactants.

$$\Delta G = m \bar{g}_M + n \bar{g}_N - a \bar{g}_A - b \bar{g}_B$$

Eq. (2.13) is substituted for each of the four terms.

$$\Delta G = m \left[g_M^{-0} + nRT \ln \left(\frac{P_M}{P_0} \right) \right] + n \left[g_N^{-0} + nRT \ln \left(\frac{P_N}{P_0} \right) \right] - a \left[g_A^{-0} + nRT \ln \left(\frac{P_A}{P_0} \right) \right] - b \left[g_B^{-0} + nRT \ln \left(\frac{P_B}{P_0} \right) \right]$$

The standard Gibbs energy terms can be consolidated into the change in standard Gibbs energy, ΔG^0 .

$$\Delta G^0 = m g_M^{\bar{0}} + n g_N^{\bar{0}} - a g_A^{\bar{0}} - b g_B^{\bar{0}}$$

The reference pressure, P^0 , is usually taken as 1 atm, and the expression can be simplified to

$$\Delta G_2 = \Delta G^0 + RT \ln \left(\frac{P_M^m P_N^n}{P_A^a P_B^b} \right)$$

Substituting Q as the general reaction quotient for the pressures,

$$Q = \left(\frac{P_M^m P_N^n}{P_A^a P_B^b} \right)$$

the expression is simplified into Eq. (2.14) for the change in Gibbs energy of a reaction involving gases.

$$\Delta G = \Delta G^0 + RT \ln Q \quad (2.14)$$

2.3.4 The Nernst Equation

The general expression in Eq. (2.14), which was derived for gas mixtures, can be converted to an expression for electrochemical equilibrium by using the work relationship presented earlier in Eq. (2.5).

$$W_e = n_e F E \quad (2.15)$$

where W_e is the electrochemical work, n_e is the number of electrical charges (electrons or protons) transferred in the reaction, F is the charge carried by a mole of electrons (or protons), and E is the voltage difference across the electrodes. The change in Gibbs energy is equal to the negative of the electrochemical work as shown in Eq. (2.4). Substituting Eq. (2.15) into Eq. (2.4) gives Eq. (2.16).

$$\Delta G = - n_e F E \quad (2.16)$$

The same substitution is applied to the standard Gibbs energy to define the standard potential, E° , in Eq. (2.17).

$$\Delta G^0 = - n_e F E^0 \quad (2.17)$$

Substituting the values of ΔG and ΔG^0 in Eq. (2.14) gives,

$$- n_e F E = - n_e F E^0 + RT \ln Q$$

$$E = E^0 - \frac{RT}{n_e F} \ln Q \quad (2.18)$$

$$E = E^0 - \frac{2.303 RT}{n_e F} \log Q$$

If the denominator of the reaction quotient is less than the numerator, the natural log term subtracts from the standard electrode potential, lowering the performance of the fuel cell. Therefore, diluting the reactant gases will lower the maximum voltage that the cell can produce.

2.4 Working of Direct Methanol Fuel Cells (DMFC)

A conceptual design of the DLFC module, principles and functioning which resulted in several dramatic improvements in the technology, are shown here:

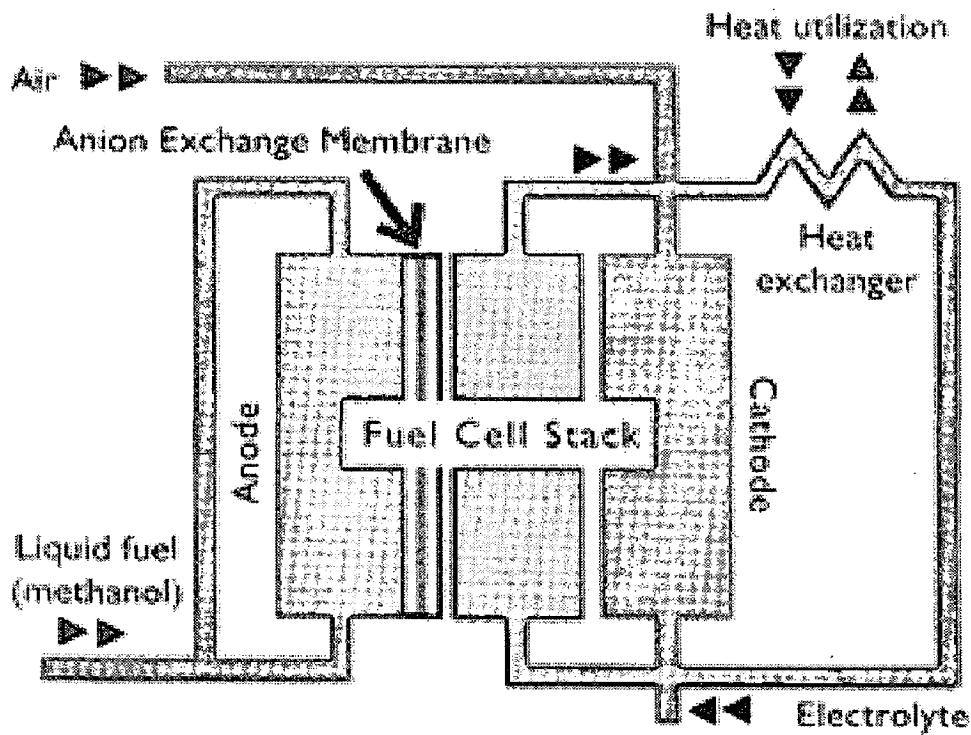


FIGURE 2.3 Design of a DLFC module

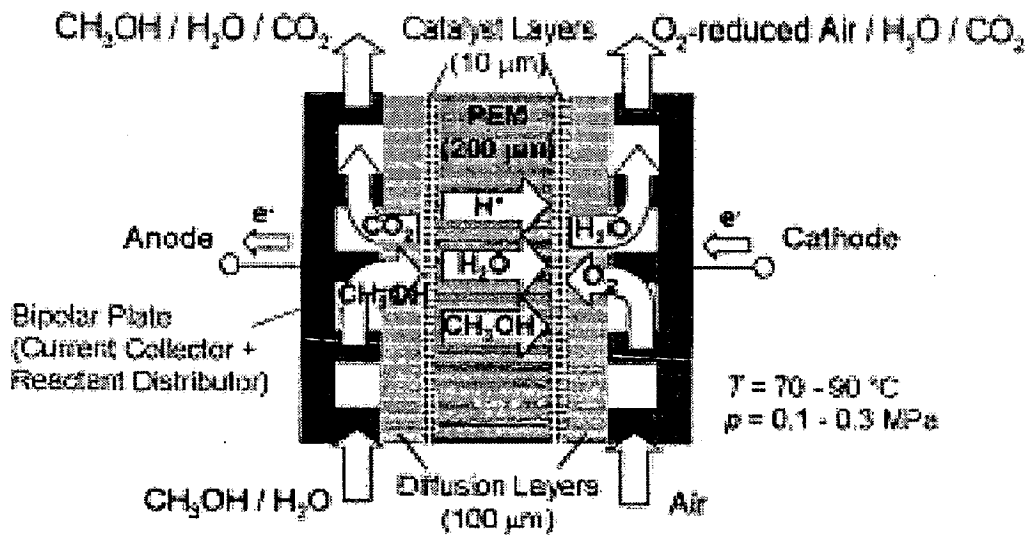


FIGURE 2.4 Reaction scheme and principle of the direct methanol fuel cell.

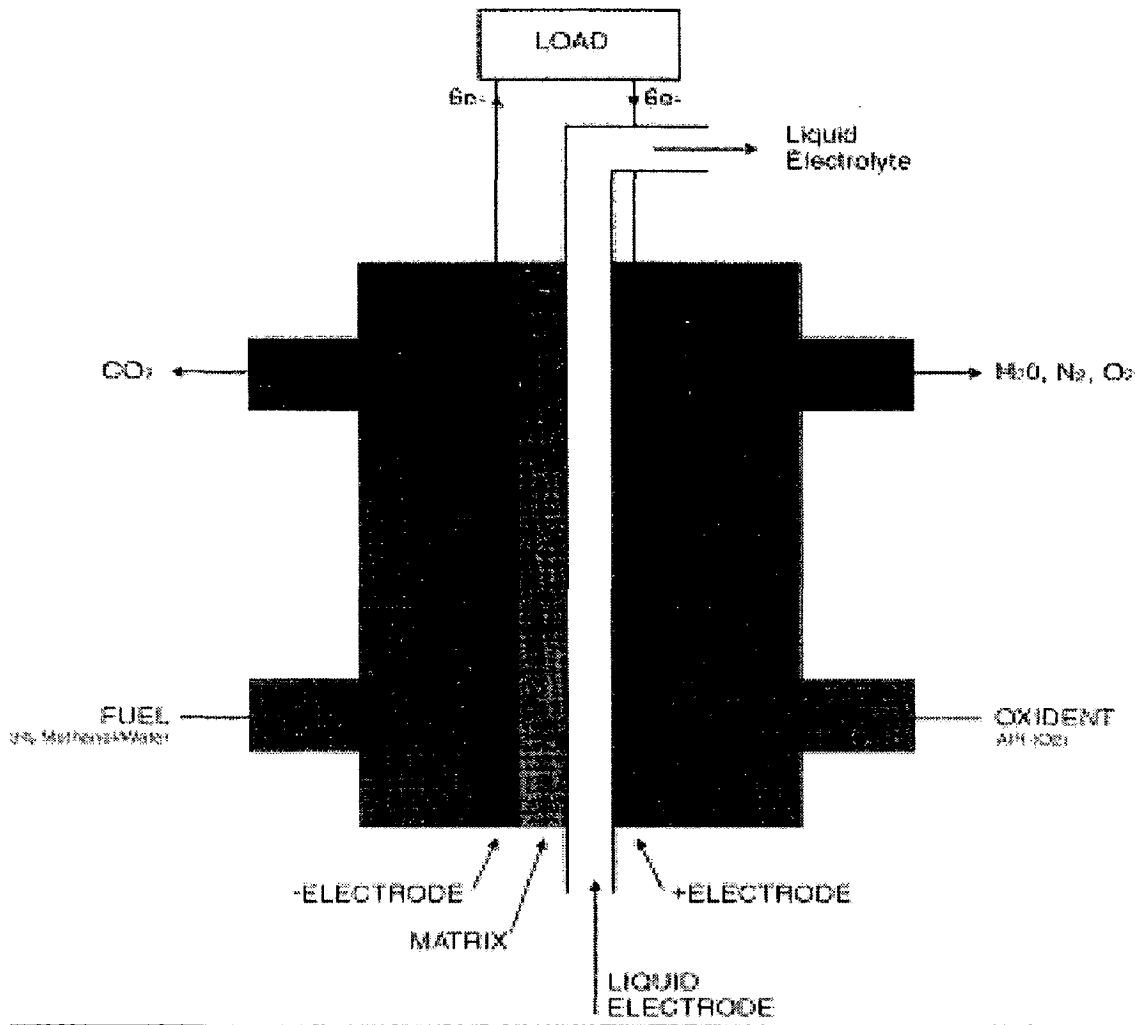


FIGURE 2.5 (a) Functioning of the direct methanol fuel cell.

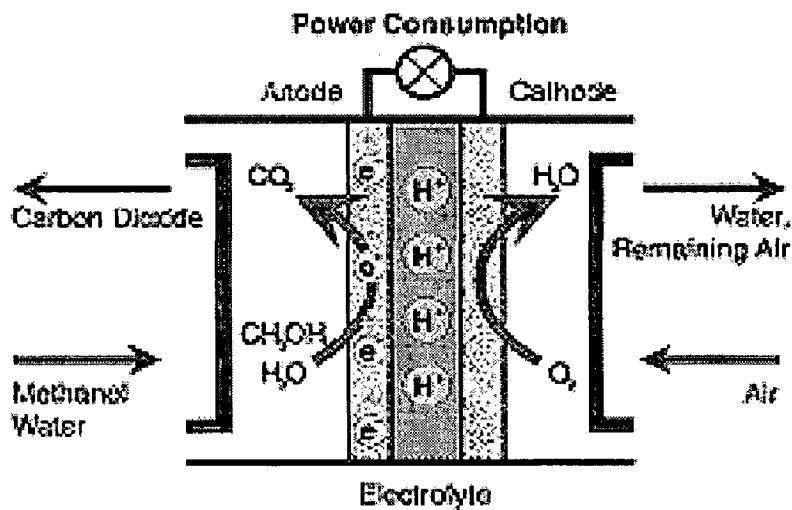


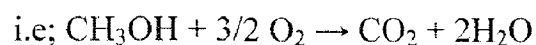
FIGURE 2.5 (b) Functioning of the direct methanol fuel cell.

2.4.1 The Direct Methanol Fuel Cell Process

The thermodynamic potential is created through the use of a polymer electrolyte membrane that allows only certain chemical species to pass through it. On one side of this membrane, a methanol and water mixture is fed to an anode catalyst that separates the methanol molecule into hydrogen atoms and carbon dioxide. The separated hydrogen atoms are then typically stripped of their electron, and passed through the membrane to the cathode side of the cell. At the cathode catalyst, the protons (hydrogen atoms without an electron) react with the oxygen in air to form water minus an electron. By connecting a conductive wire from the anode to the cathode side, the electrons stripped from the hydrogen atoms on the anode side can travel to the cathode side and combine with the electron deficient species.

From a thermodynamic perspective, the electrons "want" to travel to the cathode side a specific "amount," that can be quantified as the open circuit voltage. The open circuit voltage is measured with a voltmeter across the cell set to an extremely high resistance. The thermodynamic favoring of reacting the methanol and O₂ into carbon dioxide and water forces a difference in energy to build across the membrane until the system reaches equilibrium. Once this level is reached the components stop reacting, and no additional useful energy is produced.

Useful energy is produced by lowering the voltage across the membrane below the equilibrium value. This is done by placing a resistance on the wire connecting the two sides that is weak enough that current can flow through it. The smaller the voltage difference that is imposed on the fuel cell in this manner, the more current is produced until a proton transport rate limit is reached, after which no additional energy is produced. The overall reaction occurring in the DMFC is the same as that for the direct combustion of methanol,



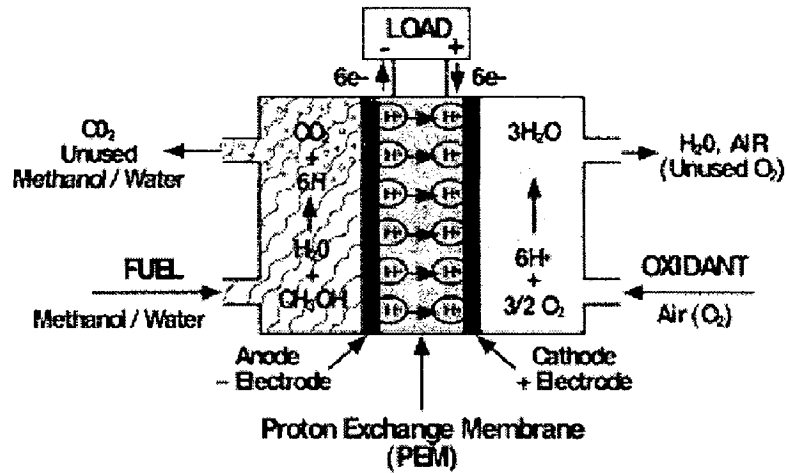


FIGURE 2.6 schematic of the operating principles of DMFC

The figure above shows a schematic of the operating principles of fuel cell utilizing methanol as fuel, i.e., a Direct Methanol Fuel Cell (DMFC). When providing current, methanol is electrochemically oxidized at the anode electrocatalyst to produce electrons which travel through the external circuit to the cathode electrocatalyst where they are consumed together with oxygen in a reduction reaction. The circuit is maintained within the cell by the conduction of protons in the electrolyte.

2.4.2 Byproducts of DMFCs

The job of the fuel cell is to convert the chemical energy of a fuel directly into electrical current without burning it. Unlike internal combustion engines there is no combustion process; therefore no airborne pollutants are generated. The only "exhaust" or by-product of this exchange is pure water and some carbon dioxide (CO₂). Unlike other fuel cell technologies, DMFC (Direct Methanol Fuel Cell) technology produces no carbon monoxide or other particulates such as oxides of nitrogen (NO_x), oxides of sulfur (SO_x) or reactive organic gases (ROG). In lay terms, the total approximate amount of carbon dioxide is **half** of what is currently generated by combustion engines. Thus, the effect on our planet of utilizing the DMFC and methanol for energy production is profound.

2.4.3 Advantages of DMFC over other fuel cells

In terms of the amount of electricity generated, a Direct Methanol Fuel Cell (DMFC) can currently generate 300-500 milli-watts per centimeter squared. The area of the cell size and the number of cells stacked together will provide the necessary power generation for whatever the watt and kilowatt needs are for vehicular and stationary applications.

The liquid fuel design of Direct Methanol Fuel Cells has numerous system-level advantages over the gas fuel or reformer design fuel cells. A Direct Methanol Fuel Cell (DMFC):

- Eliminates the fuel vaporizer or "reformer"
- Eliminates high pressures and temperatures. DMFC operate effectively at room temperature and pressures less than 20 psi.
- Eliminates the complex water and thermal management systems that are needed to maintain the equilibrium of temperature and pressures in the reformer type fuel cells.

This in turn,

- Eliminates the need for inner heating and cooling plates.
- Eliminates the humidification process of reformer technology without which membranes dry up and crack. The liquid state of Direct Methanol Fuel Cells provides a constant bath for the membranes.
- Significantly lowers system size and weight, due in large part to the elimination of the reformer, a costly, complex space hog.
- DMFCs use bi-plates that can be made out of non-metallic lightweight, flexible materials that are significantly lower in cost than metallic materials.

Mathematical Analysis and Model Development

This Chapter describes the formulation of mathematical model for liquid-feed direct methanol fuel cell.

Mathematical Analysis of the proposed model:

- Determine the Gibbs Potential of the electrochemical reaction, a *thermodynamic property* and strong function of temperature
- Determine the Nernst Potential of the electrochemical reaction *in the reaction conditions*. The Nernst Potential is equal to the Gibbs Potential minus a correction for the partial pressures of reactants in the electrochemical reaction.
- Determine the cell voltage with the specified cell *materials*.

Input: Temperature, Pressure

Output: Gibbs Potential, ΔH , ΔG , W_{Net} , i_{density} , V_{cell} , η_{th}

3.1 Model Development

Based on the principles of fuel cells performance, and in order to calculate thermal and electrical output, following Mathematical Model for fuel cell performance assessment can be suggested. The model is based on electrochemical engineering fundamentals and has been developed on the following assumptions:

Assumptions:

- Fuel and oxidant are perfect gases.
- The model can be applied on any type of fuel cells.
- It considers stationary fuel cells.
- The fuel is CH_3OH i.e. 3% Methanol/Water; and the oxidant is O_2 .
- The conversion of energy occurs isothermally and in constant volume.
- Temperature and pressure are uniform along the electrodes.
- Adiabatic operation – reasonable. Stack is assumed to be effectively insulated.
- Total Air side molar flow unchanged for K_p calculation.
- K_p independent of pressure – true if Ideal Gas approximation holds.

- Degree of conversion is assumed to be 99%
- Physical geometry is assumed to be rectangular.
- Cell active area is assumed to be 5 cm²

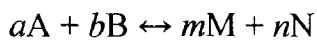
3.1.1 Calculation Stages

The following steps have been identified for modeling:

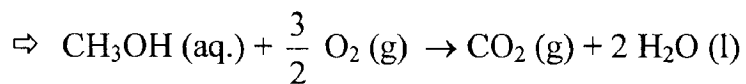
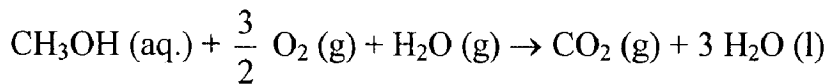
Step – 1:

Define the chemical reaction equations and the corresponding stoichiometric coefficients

General Equation:



In our case:

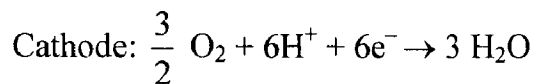
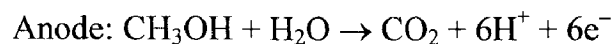


Comparing the two gives,

$$a = 1, b = 3/2, m = 1 \text{ and } n = 2.$$

Step – 2:

Define the half reactions at the anode and cathode and the *valency*, n_e :

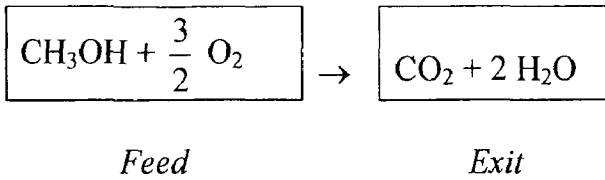


Thus, number of $\text{e}^- = n_e = 6$ (in our case)

Step - 3:

Establish the operating temperature, T, and partial pressures, p_{CO_2} , $p_{\text{H}_2\text{O}}$, $p_{\text{CH}_3\text{OH}}$, p_{O_2} , of the reaction components.

Our reaction is:



Having, partial pressure = Total pressure x Mole fraction

The partial pressures of the reaction components are calculated as:

Reaction Component	No. of moles in Feed	No. of moles at exit	Mole fraction at exit
CO ₂	0	ε	ε/0.5 (ε + 5)
H ₂ O	0	2 ε	2 ε/0.5 (ε + 5)
CH ₃ OH	1	1 - ε	(1 - ε) / 0.5 (ε + 5)
O ₂	3/2	3/2 (1 - ε)	3/2 (1 + ε) / 0.5 (ε + 5)

where, ε is 'degree of conversion'

Thus,

$$p_{\text{CO}_2} = P \cdot \frac{\varepsilon}{0.5(\varepsilon + 5)},$$

$$p_{\text{H}_2\text{O}} = P \cdot \frac{2\varepsilon}{0.5(\varepsilon + 5)},$$

$$p_{\text{CH}_3\text{OH}} = P \cdot \frac{(1 - \varepsilon)\varepsilon}{0.5(\varepsilon + 5)}, \text{ and}$$

$$p_{\text{O}_2} = P \cdot \frac{\frac{3}{2}(1 - \varepsilon)}{0.5(\varepsilon + 5)}$$

where, P = Total pressure.

Step – 4:

Establish the equilibrium constant 'K' at operating temperature (the) and pressure (P).

$$K = K_y \cdot K_\phi P^{(v_i)}$$

where,

K_y = equilibrium constant of mole fractions

K_ϕ = equilibrium constant of fugacity coefficients

P = Total pressure

v_i = degree of freedom of reaction

In case of liquid-feed DMFC,

$$K_y = \frac{[p_{CO_2}]x[p_{H_2O}]^2}{[p_{CH_3OH}]x[p_{O_2}]^{\frac{3}{2}}}$$

Thus,

$$K = \frac{[p_{CO_2}]x[p_{H_2O}]^2}{[p_{CH_3OH}]x[p_{O_2}]^{\frac{3}{2}}} \cdot K_\phi P^{(v_i)}$$

Step – 5:

a.) Calculate the Gibbs free energy at standard temperature and pressure

(T = 25 °C / 298 K; P = 1 atm)

$$\Delta G_{rxn,298}^0 = \Delta G_{rxn,298}^0 [products] - \Delta G_{rxn,298}^0 [reactants]$$

For a DMFC,

$$\Delta G_{rxn,298}^0 = \{\Delta G_{rxn,298}^0 [CO_2] + 2 \Delta G_{rxn,298}^0 [H_2O]\} - \{\Delta G_{rxn,298}^0 [CH_3OH] + \frac{3}{2} \Delta G_{rxn,298}^0 [O_2]\}$$

b.) Calculate the Gibbs free energy at specific temperature (T) and pressure (P)

$$\Delta G_{rxn,T} = \Delta G_{rxn,298}^0 + RT \ln[K]$$

$$K = \frac{[p_{CO_2}]x[p_{H_2O}]^2}{[p_{CH_3OH}]x[p_{O_2}]^{\frac{3}{2}}} \cdot K_{\phi}P^{(\nu_i)} \quad (\text{For DMFC})$$

Thus,

$$\Delta G_{rxn,T} = \Delta G_{rxn,298}^0 + RT \ln \left[\frac{[p_{CO_2}]x[p_{H_2O}]^2}{[p_{CH_3OH}]x[p_{O_2}]^{\frac{3}{2}}} \cdot K_{\phi}P^{(\nu_i)} \right]$$

Step – 6:

a.) Calculate of change in Enthalpy at standard temperature and pressure

$$\Delta H_{rxn,298}^0 = \Delta H_{rxn,298}^0 [\text{products}] - \Delta H_{rxn,298}^0 [\text{reactants}]$$

For a DMFC,

$$\Delta H_{rxn,298}^0 = \{ \Delta H_{rxn,298}^0 [CO_2] + 2 \Delta H_{rxn,298}^0 [H_2O] \} - \{ \Delta H_{rxn,298}^0 [CH_3OH] + \frac{3}{2} \Delta H_{rxn,298}^0 [O_2] \}$$

b.) Calculate the change in Enthalpy at specific temperature (T).

$$\Delta H_{rxn,T} = \Delta H_{rxn,298}^0 + R \left[\Delta A (T-298) + \frac{\Delta B}{2} (T^2-298^2) + \frac{\Delta C}{3} (T^3-298^3) - \frac{\Delta D}{1} \left(\frac{1}{T} - \frac{1}{298} \right) + \frac{\Delta E}{4} (T^4-298^4) \right]$$

where,

$$\Delta A = A [\text{products}] - A [\text{reactants}]$$

For a DMFC,

$$\Delta A = \{ [A_{CO_2}] + 2 [A_{H_2O}] \} - \{ [A_{CH_3OH}] + \frac{3}{2} [A_{O_2}] \}$$

Similarly, values of ΔB , ΔC , ΔD , ΔE would be established.

Step – 7:

a.) Establish the standard fuel cell EMF

$$\Delta G_{rxn,298}^0 = -n_e F E^0$$

$$\Rightarrow E^0 = - \frac{\Delta G_{rxn,298}^0}{n_e F}$$

where,

F = Faraday's constant

b.) Establish the Nernst potential at a specific temperature (T) and pressure (P = 1 atm)

$$E_{Nernst} = E^0 - \frac{2.303 RT}{n_e F} \log Q$$

where, Q is the general reaction quotient for the pressures, and equals

$$Q = \frac{[p_{CO_2}]^x [p_{H_2O}]^2}{[p_{CH_3OH}]^x [p_{O_2}]^2} \quad (\text{for DMFC})$$

Step – 8:

Establish the maximum work output of the fuel cell.

For a fuel cell, in electrical terms, the work done by electrons with the charge $n_e F$ moving through a potential difference, E is:

$$W_{cell} = n_e F E$$

$$\text{Also, } \Delta G_{rxn,T} = -n_e F E$$

Thus,

$$W_{cell} = - \Delta G_{rxn,T}$$

Step – 9:

Establish the fuel cell heat output

$$Q_P = \Delta H_{rxn,298}^0$$

where,

$\Delta H_{rxn,298}^0 = H_P - H_R$, is the change in enthalpy of formation

Step – 10:

Establish the fuel cell thermal efficiency.

$$\eta_{th} = \frac{W_{cell}}{Q_P}$$

Step – 11:

Establish the cell current and current density.

$$I = n_c n_e F$$

where,

n_c = fuel rate in gm-moles / sec

$$I_{density} = I / A$$

where, A is the available area in cm^2

Step – 12:

Establish the cell voltage.

The cell voltage is given by application of Ohms Law ($R = V/I$)

$$V_{cell} = E_{Nernst} - I_{density} \times ASR_{cell}$$

Where $I_{density}$ is the current density of the electrochemical reaction, and ASR_{cell} is the Area Specific Resistance of the cell i.e. the resistance seen by the current density.

Solution of the Model

This chapter presents an algorithm of the method to solve the model equations described in the previous chapter. To initiate the calculations, values for 'degree of conversion', 'fuel flow rate', 'cell geometry specifications' and 'area specific resistance' are assumed.

4.1 Solution of thermodynamic equations

Based on inlet data and assumed parameters, as suggested in the algorithm, Fig. 4.1, the solution first requires the calculation of partial pressures of reaction components. For liquid-feed direct methanol fuel cell, they are as follows:

$$p_{CO_2} = P \cdot \frac{\varepsilon}{0.5(\varepsilon + 5)},$$

$$p_{H_2O} = P \cdot \frac{2\varepsilon}{0.5(\varepsilon + 5)},$$

$$p_{CH_3OH} = P \cdot \frac{(1 - \varepsilon)\varepsilon}{0.5(\varepsilon + 5)}, \text{ and}$$

$$p_{O_2} = P \cdot \frac{\frac{3}{2}(1 - \varepsilon)}{0.5(\varepsilon + 5)}$$

For solving the model, we have optimized the model by assuming the degree of conversion, $\varepsilon = 99\%$

The partial pressures thus calculated would be substituted in the relevant equation to calculate the Equilibrium Constant, K, at varying P and T.

$$K = \frac{[p_{CO_2}] \times [p_{H_2O}]^2}{[p_{CH_3OH}] \times [p_{O_2}]^{\frac{3}{2}}} \cdot K_{\phi} P^{(v_i)}$$

Since the model is optimized with an assumption that ideal gas scenario is applicable,

$$K_{\phi} = 1$$

Thus,

$$K = \frac{[p_{CO_2}] \times [p_{H_2O}]^2}{[p_{CH_3OH}] \times [p_{O_2}]^{\frac{3}{2}}} \cdot P^{(v_i)}$$

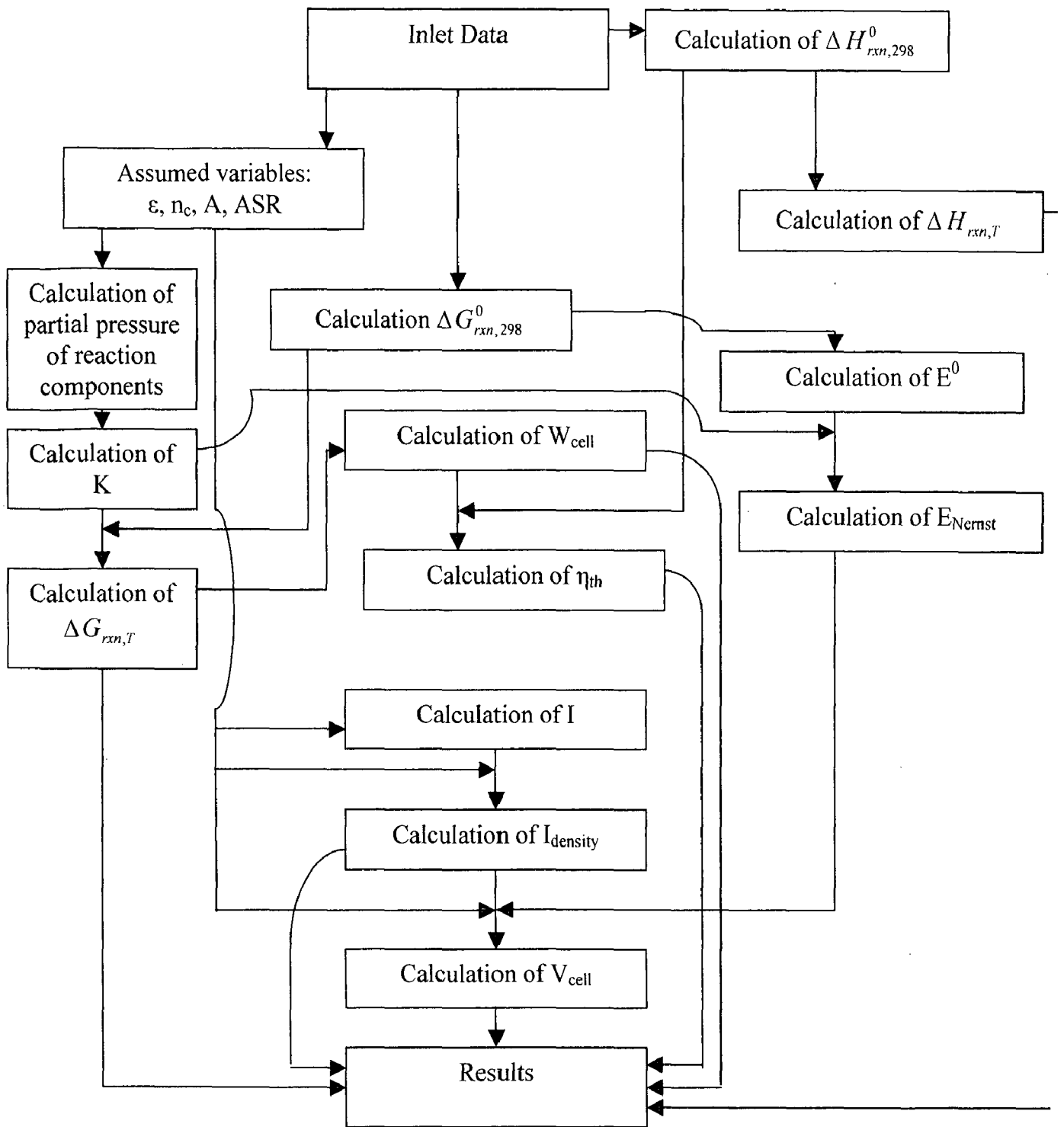


FIGURE 4.1 Algorithm for solution of model

Also, the value of $\Delta G_{rxn,298}^0$ is calculated from the inlet data.

Having calculated the values of K and $\Delta G_{rxn,298}^0$, $\Delta G_{rxn,T}$ is calculated subsequently, using

$$\Delta G_{rxn,T} = \Delta G_{rxn,298}^0 + RT \ln[K]$$

Having known $\Delta G_{rxn,T}$ here will also establish the values of W_{cell} , as

$$W_{cell} = - \Delta G_{rxn,T}$$

Next to this, $\Delta H_{rxn,298}^0$ and $\Delta H_{rxn,T}$ solved and the solution involves the data from the standard thermodynamic property tables.

$$\Delta H_{rxn,298}^0 = \{ \Delta H_{rxn,298}^0 [\text{CO}_2] + 2 \Delta H_{rxn,298}^0 [\text{H}_2\text{O}] \} - \{ \Delta H_{rxn,298}^0 [\text{CH}_3\text{OH}] + \frac{3}{2} \Delta H_{rxn,298}^0 [\text{O}_2] \}$$

Also,

$$Q_P = \Delta H_{rxn,298}^0$$

Thus, Q_P is also obtained with the calculation of $\Delta H_{rxn,298}^0$

$$\Delta H_{rxn,T} = \Delta H_{rxn,298}^0 + R \left[\Delta A (T-298) + \frac{\Delta B}{2} (T^2-298^2) + \frac{\Delta C}{3} (T^3-298^3) - \frac{\Delta D}{1} \left(\frac{1}{T} - \frac{1}{298} \right) + \frac{\Delta E}{4} (T^4-298^4) \right]$$

Having calculated the value of $\Delta G_{rxn,298}^0$ in the previous step, gives E^0 as:

$$E^0 = - \frac{\Delta G_{rxn,298}^0}{n_e F}$$

where F = Faraday's constant = = 96485 C / (mole e⁻)

Specifically, at P = 1 atm

$$Q = K = \frac{[p_{CO_2}]x[p_{H_2O}]^2}{[p_{CH_3OH}]x[p_{O_2}]^2}$$

Having known E^0 and Q , E_{Nernst} is calculated as:

$$E_{Nernst} = E^0 - \frac{2.303 RT}{n_e F} \log Q$$

Also, having the known the values of W_{cell} and Q_p

$$\eta_{th} = \frac{W_{cell}}{Q_p}$$

Further to this, current and current density are established.

n_c is assumed over a range

For a DMFC,

$$n_e = 6$$

Thus,

$$I = 578910n_c$$

Coming to the current density, the geometric dimensions are required which are again assumed as one of the design parameter.

The design parameters are assumed as:

Geometry: rectangular

$$\text{Cell active area} = 5 \text{ cm}^2$$

Thus,

$$\begin{aligned} I_{\text{density}} &= I / A \\ &= 121571.1n_c \end{aligned}$$

Having known E_{Nernst} and I_{density} , finally the cell voltage is calculated as

$$V_{\text{cell}} = E_{\text{Nernst}} - I_{\text{density}} \times \text{ASR}_{\text{cell}}$$

$$\Rightarrow V_{\text{cell}} = E_{\text{Nernst}} - 121571.1 n_c \times \text{ASR}_{\text{cell}}$$

The model is optimized with ASR_{cell} assumption as:

$$\text{ASR}_{\text{cell}} = 4.737 \Omega\text{-cm}^2$$

This gives,

$$V_{\text{cell}} = E_{\text{Nernst}} - 575882.3 n_c$$

Finally, all the output parameters, which are calculated, are tabulated for further graphical representation, analysis and subsequent validation

Results and Discussion

The mathematical model is developed. This chapter describes the results obtained by solving the model developed in chapter 3. The model was solved using the algorithm explained in chapter 4 for mathematical modeling of liquid-feed direct methanol fuel cell. Net work output, net heat output, thermal efficiency, Nernst potential and cell voltage are calculated for DMFC. The sample calculation of one set of parameters has been given in Annexure-B.

In the following section, model validity and effect of operation variables, namely temperature, pressure and fuel flow rate, has been analyzed.

In this study, the operating parameters are optimized in accordance with the reference model proposed by *Z. H. Wang* and *C. Y. Wang*¹ and are given below in Table 5.1. Also, validation is made by comparing the two models.

Further, this chapter describes the variation of operating variables on thermodynamic and electrochemical properties of DMFC.

Table 5.1 Operating Parameters

Parameter	Value
Temperature	25 °C – 90 °C
Pressure	1 – 5 atmosphere
Degree of conversion, ϵ	99%
Fuel Flow Rate, n_c	$2.15 \times 10^{-7} - 2.33 \times 10^{-6}$ gm-mole/sec
Cell Active Area	5 cm ²
Area Specific Resistance	4.737 Ω - cm ²

The variation of Gibbs free energy as a function of temperature at different values of pressure is calculated and shown in Fig. 5.1. This provides us with the trend in the variation of the net work output of the fuel cell as a function of temperature. The change

in enthalpy of a reaction is indicative of the net heat output. The trend of the variation in net heat output as a function of temperature is analyzed by analyzing the change in enthalpy curve as a function of temperature, as shown in Fig. 5.2.

The variation of thermal efficiency of the concerned fuel cell as a function of operating temperature is shown in Fig. 5.3. Nernst potential, an inherent electrochemical property of a fuel cell is analyzed at varying temperatures in Fig. 5.5. Also, the effect of variation in fuel flow rate on cell current is represented in the Fig. 5.6.

Fuel cell *polarization curve* is drawn between cell voltage and current density in Fig. 5.7 and is the main characteristic curve for validation of proposed model against the reference model.

5.1 Validity of Model

Polarization curves for the baseline cell as proposed in the model developed by *Z. H. Wang* and *C. Y. Wang*¹ is shown below:

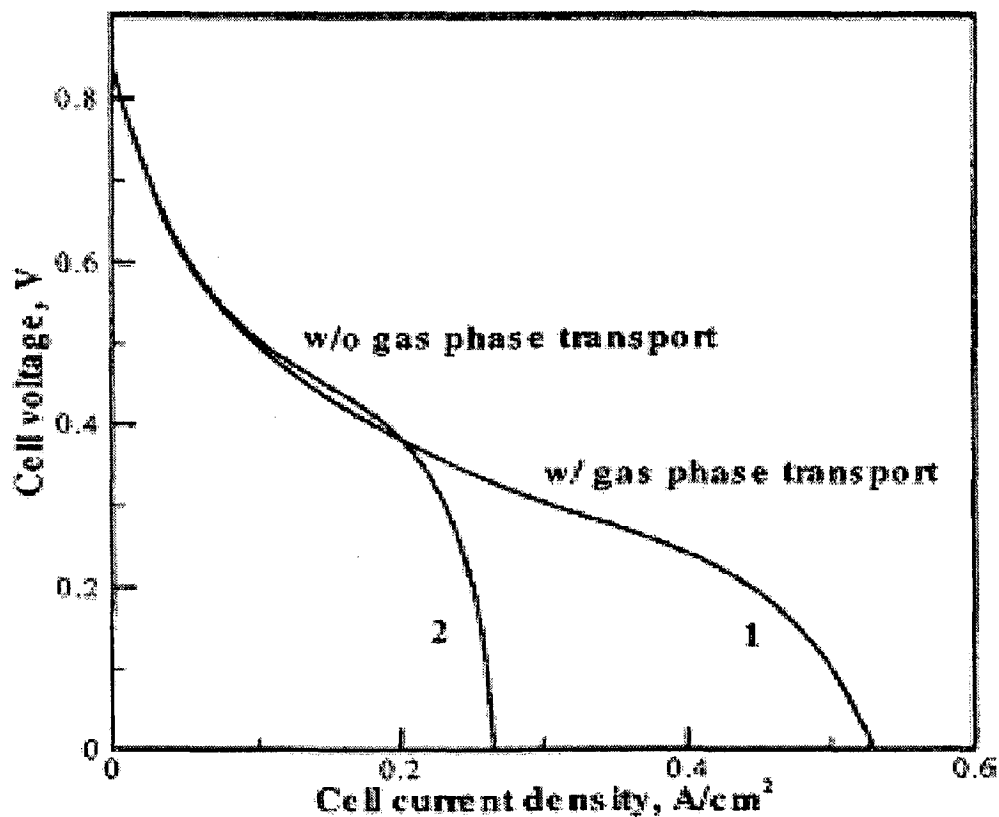


Fig. 5.7 reveals the *Polarization curve* for the liquid-feed direct methanol fuel cell as proposed in the model developed under this dissertation:

Graphical comparison of the two curves, ignoring the transport phenomena involved, is indicative of the curvature similarity between the two curves and hence, validates the proposed model. A near similarity is observed in the values of cell voltage corresponding to a specific current density, on comparison of the proposed model with the reference model.

From the polarization curve of the reference model suggested by *Z. H. Wang* and *C. Y. Wang*¹, following values are extracted using the software, 'Data from Graph':

Table 5.2 Model Validation

Current Density, A/cm²	Cell Voltage - Proposed Model	Cell Voltage – Reference Model	Variation, %
0.25	0.2	0.198	≈10%
0.175	0.4	0.423	≈5%
0.05	0.6	0.608	≈1%
0.025	0.7	0.707	≈1%

A near similarity is observed in the values of cell voltage corresponding to a specific current density, on comparison of the proposed model with the reference model. The variation in values between the reference model and the proposed model range between 1 – 10 %, which is suitable acceptable range.

Hence, the proposed model is validated along with the assumptions.

5.2 Effect of Variables

Calculations have been performed for the different range of different variables given in Table 5.1.

Calculation for the output variables namely, fuel cell efficiency, net work output, net heat output, Nernst potential and cell voltage, has been done as the procedure given in Annexure-B and results in Annexure-C.

Following sub-sections discuss the effect of operating variables, namely, temperature, pressure, fuel flow rate on the output variables.

5.2.1 Effect of temperature

Close examination of the figures reveal following features:

- Fig. 5.4. reveals that net work output at a specific pressure increases with increase in temperature
- Fig. 5.2 reveals that net heat output of a fuel cell decreases with increase in fuel cell operating temperature
- Fig. 5.3 reveals that thermal efficiency of a fuel cell increases with increase in fuel cell operating temperature. Although the degree of increase in the thermal efficiency is higher at higher temperature range.
- Fig. 5.5 reveals that Nernst potential of a fuel cell increases with increase in fuel cell operating temperature. The degree of increase of Nernst potential with temperature closely resembles the exponential curve.

5.2.2 Effect of pressure

- Fig. 5.4. reveals that net work output at a specific pressure increases with increase in temperature. However, the value of net work output lowers with increasing operating pressure.
- All other output parameters are established at fixed pressure of 1 atm and the effect of the pressure therewith is considered to be negligible.

5.2.3 Effect of fuel flow rate

- Fig. 5.4. reveals that the cell current is directly proportional to the fuel flow rate thus indicative of the increase in cell current with increase in fuel flow rate.

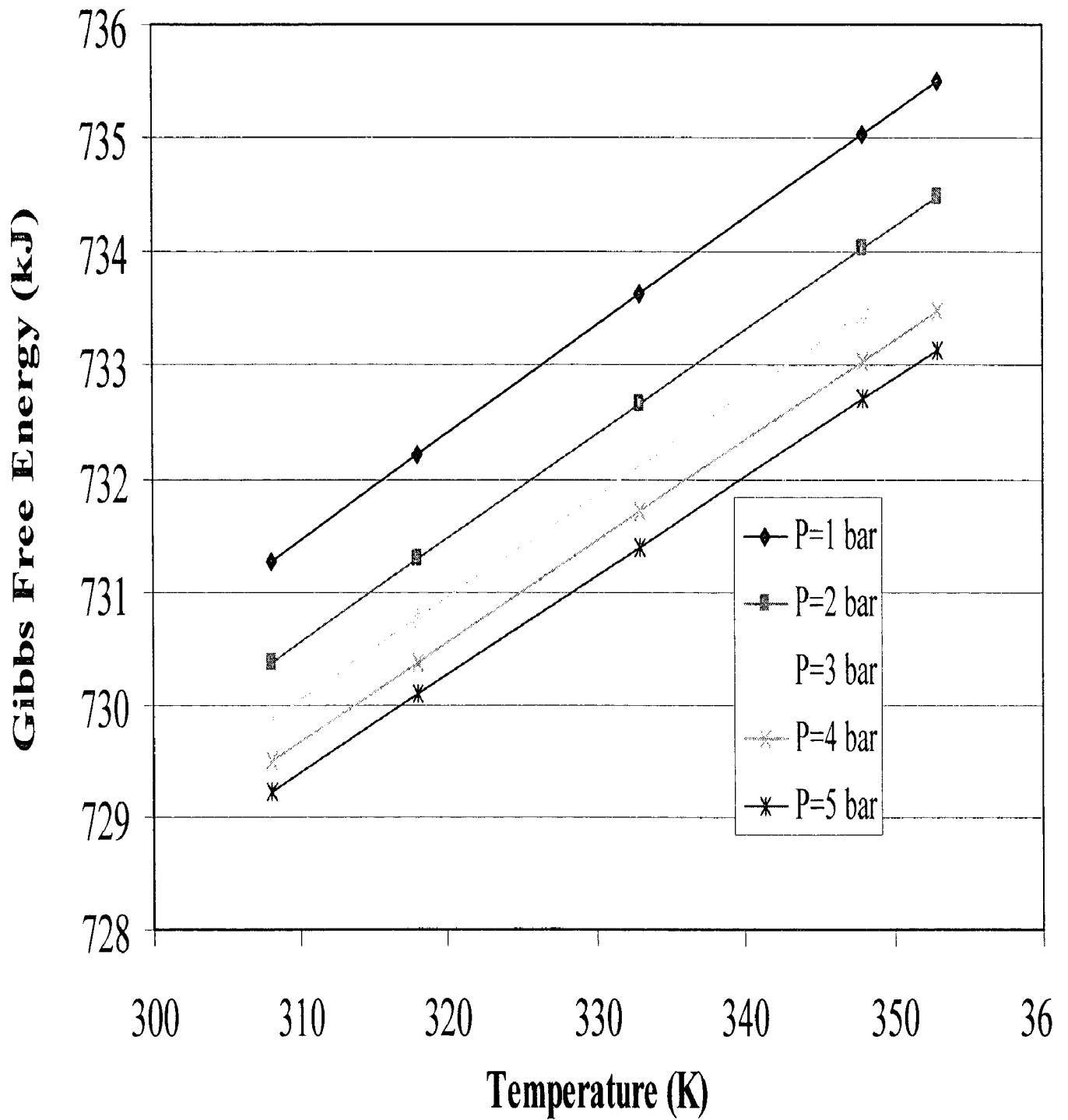


Fig. 5.1 shows the variation of Gibbs free energy as a function of temperature for different values of pressure

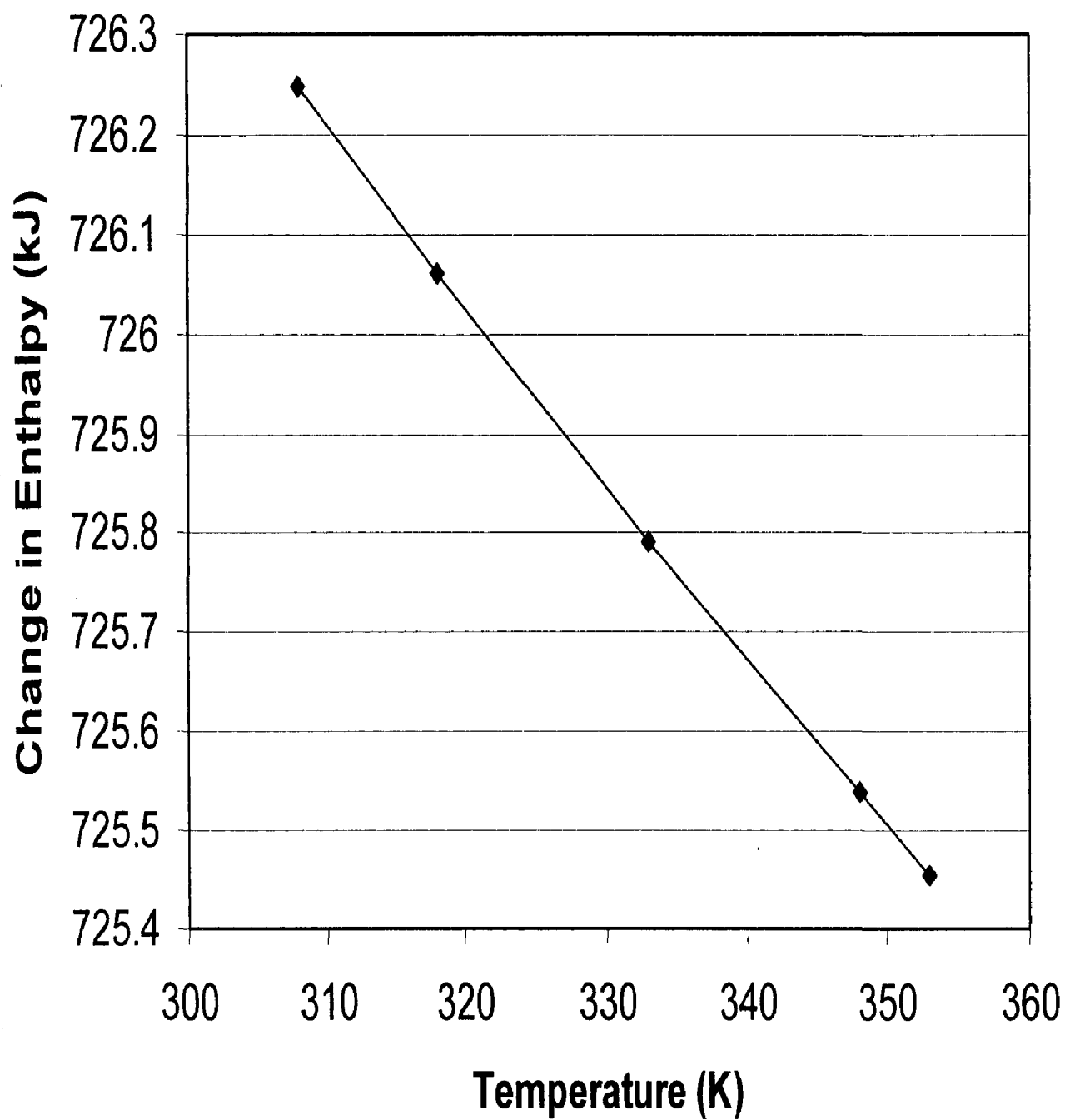


Fig. 5.2 Change in Enthalpy vs. Temperature

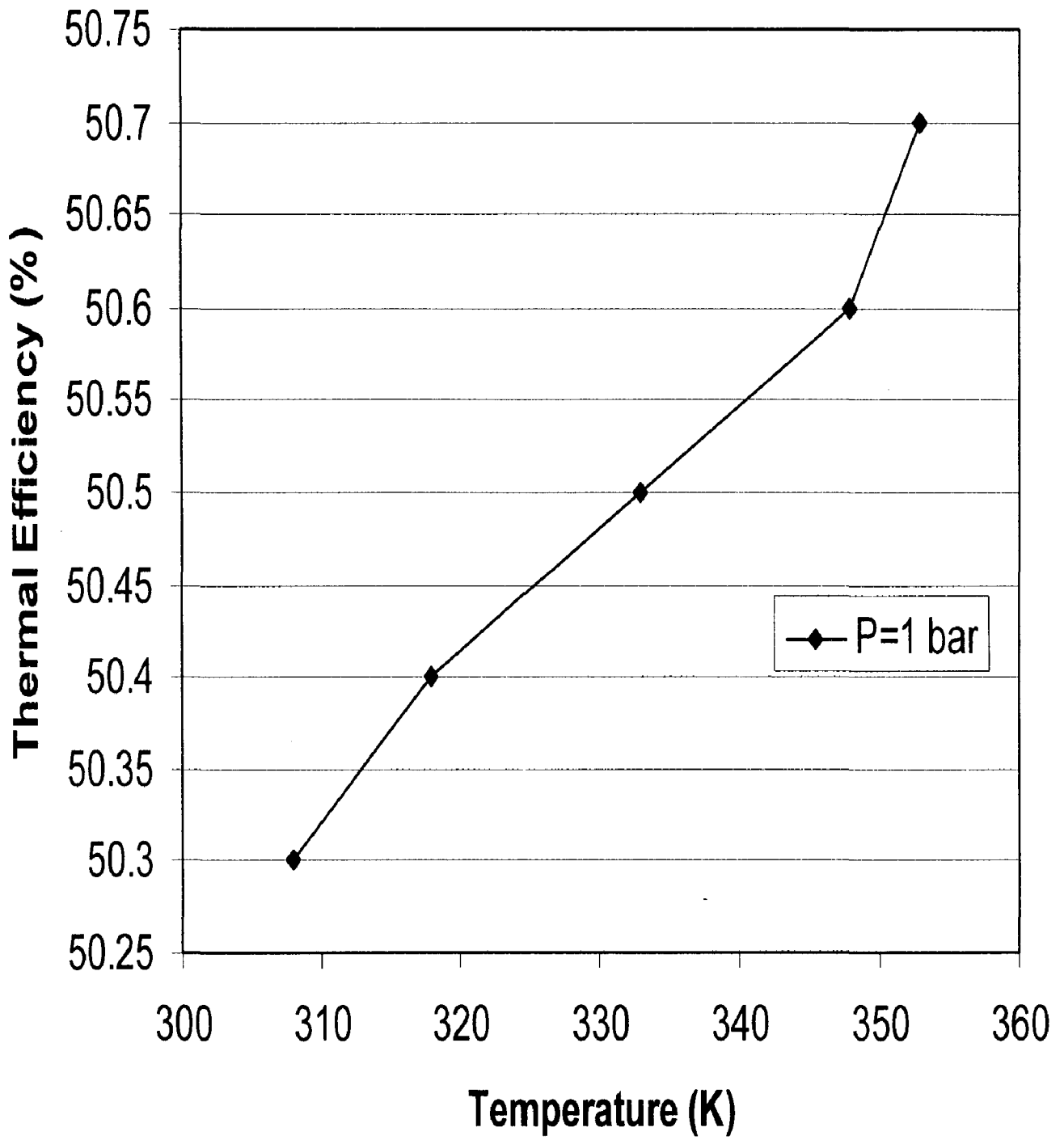


Fig. 5.3 Thermal Efficiency vs. Temperature

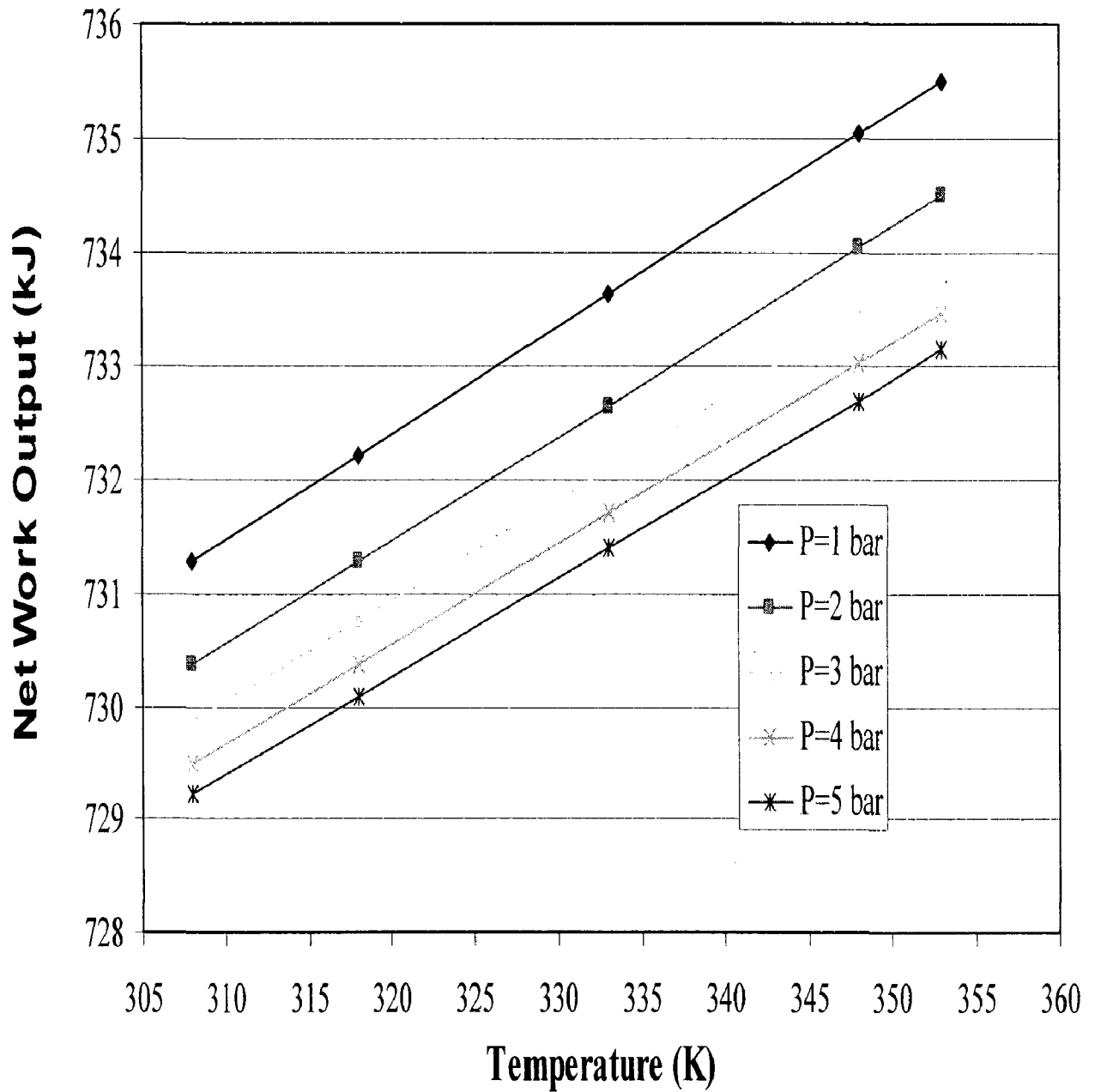


Fig. 5.4 shows the variation of Net Work Output (W_{net}) as a function of temperature for different values of pressure

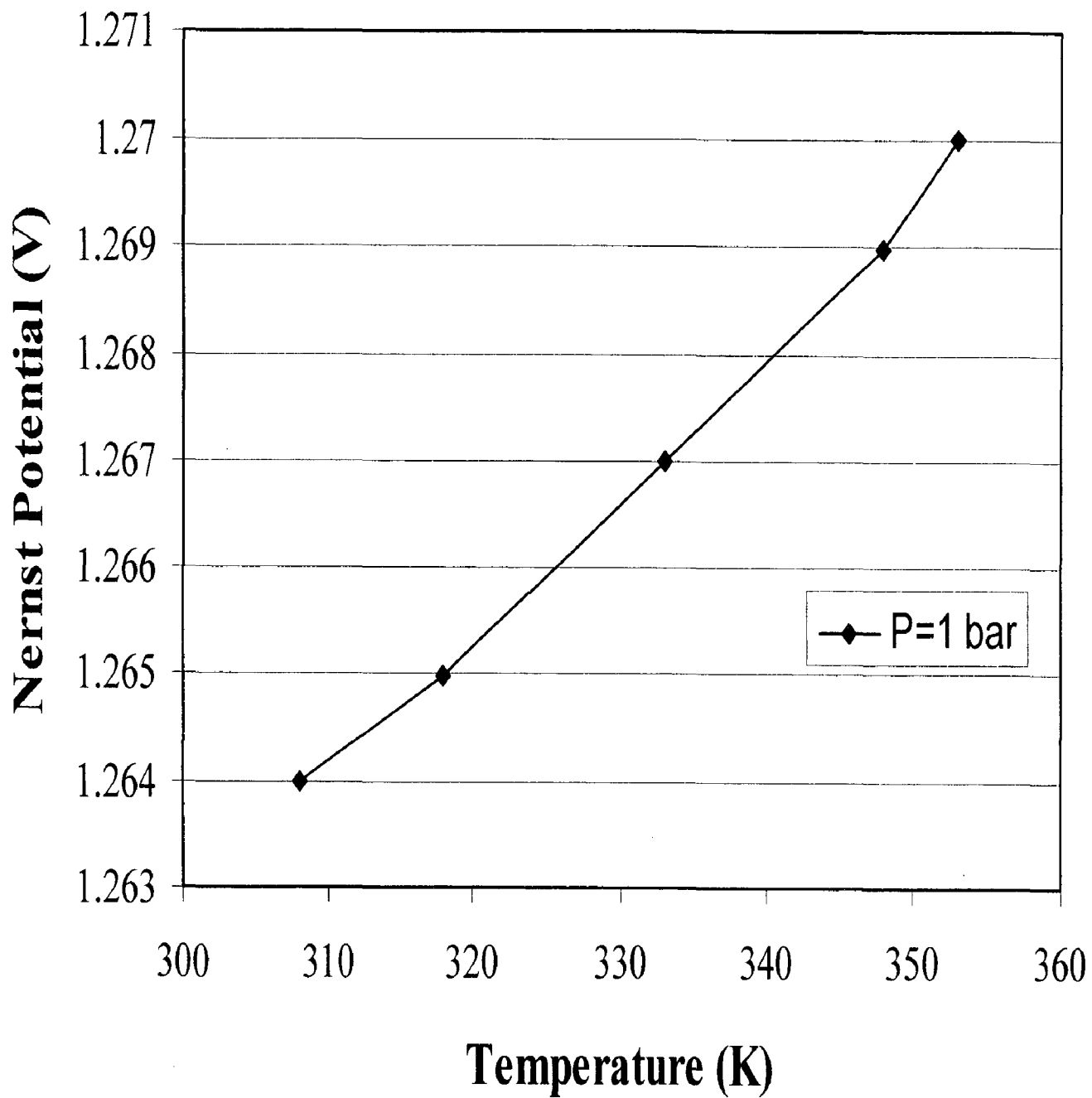


Fig. 5.5 Nernst Potential vs. Temperature

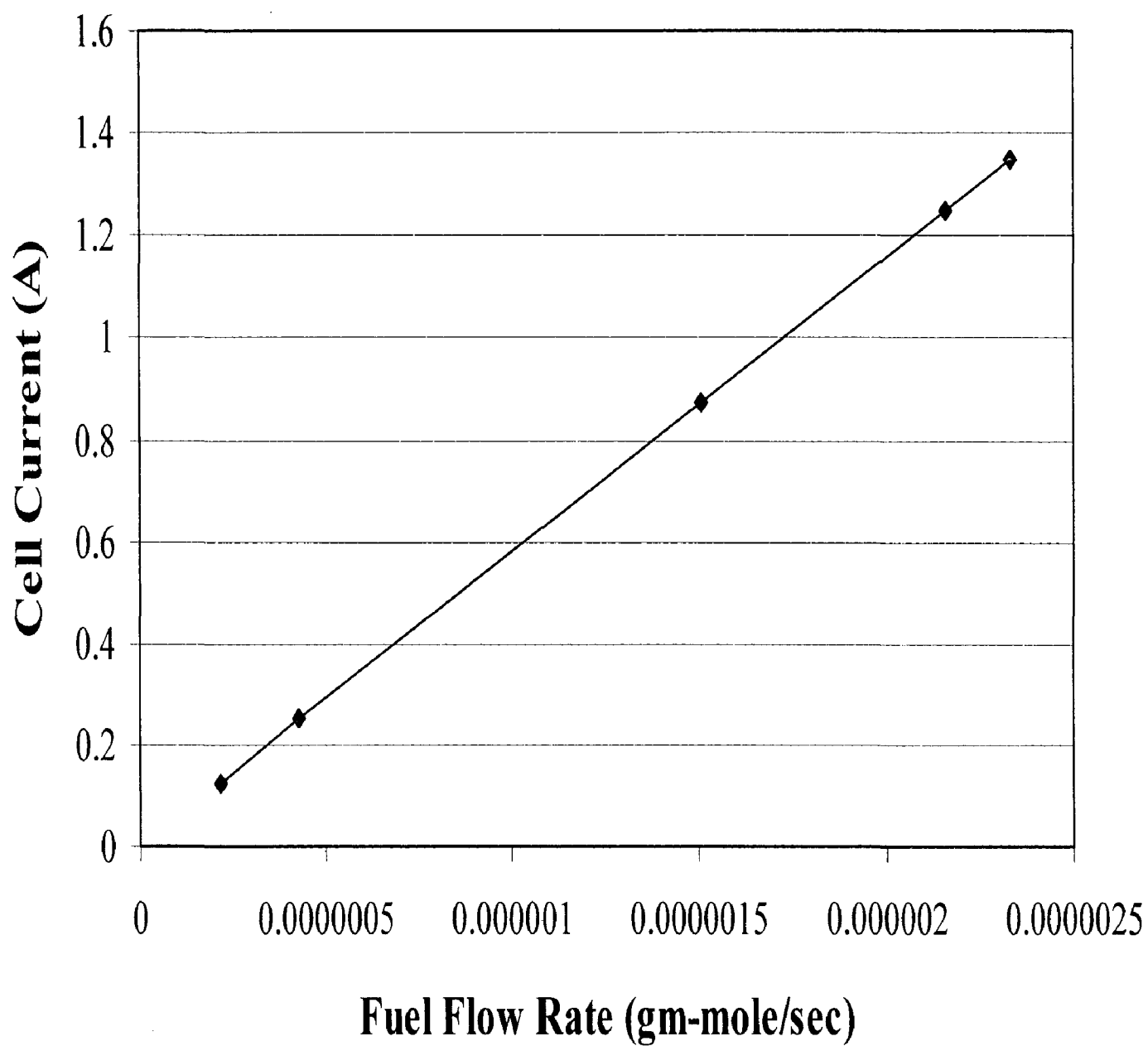


Fig. 5.6 Cell Current vs. Fuel Flow Rate

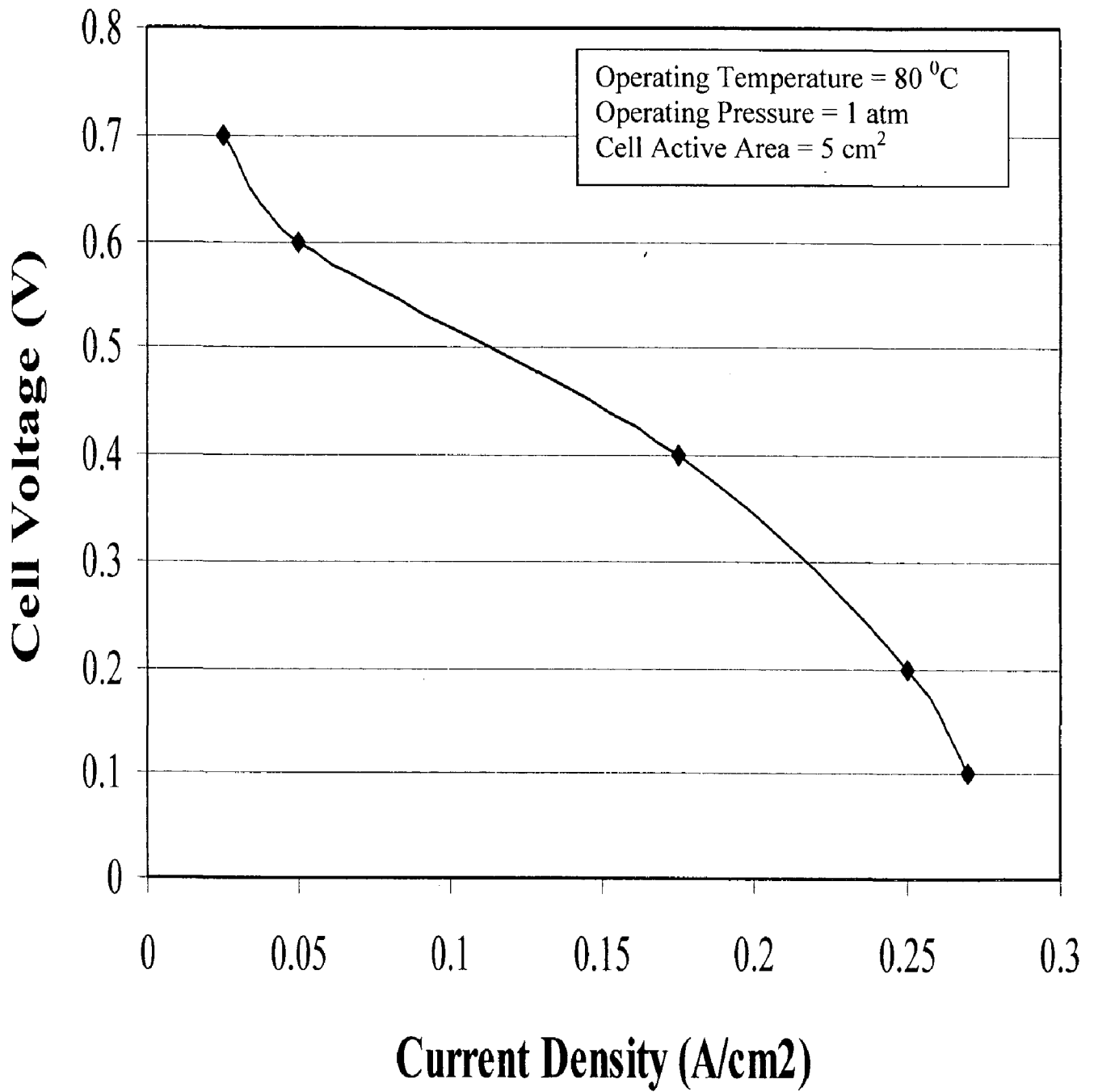


Fig. 5.7 Cell Voltage vs. Current Density

Conclusion and Recommendations

6.1 Conclusion

Following conclusions can be drawn using the results obtained in chapter 5:

1. The increase in methanol feed flow rate leads to a proportional increase in the maximum current density which in turn leads to decrease in cell voltage.
2. Nernst potential is observed to dependent on temperature and increases with increase in temperature. Also, as established in the proposed model, the cell voltage is affected with the increase or decrease in cell potential. Having kept the fuel flow rate steady at a specific cell active area and area specific resistance, it can be concluded that increase in temperature will increase the cell voltage.
3. The thermal efficiency, which is a contributing factor in the total efficiency of the cell, increases with increase in temperature. Also, the degree of conversion is assumed to be high which gives high net heat output and high work output.
4. The mathematical model developed has shown satisfactory results in simulating a liquid-feed direct methanol fuel cell. The results have been found to agree with those of *Z. H. Wang* and *C. Y. Wang*¹. The maximum deviation found is of the order of 10%.
5. The model and its solution has also been successful in determining the effect of various operating variables.

6.2 Recommendations

Although this model and the suggested algorithm for the solution of the model has been able to simulate the liquid-feed direct methanol fuel cell within satisfactory limits, still many of simplifications, which exists now could be rectified and are henceforth being recommended here for further investigation.

1. In this study, a very high degree of conversion has been assumed which is not the actual case. Methanol crossover is observed in real working situations. The cell voltage is greatly reduced due to excessive methanol crossover and the maximum cell current density may be limited by oxygen transport on the cathode because the parasitic reaction of crossed methanol consumes oxygen

as well. So a study can be made by taking a model that include the effects of methanol crossover to obtain more accurate and practically applicable results.

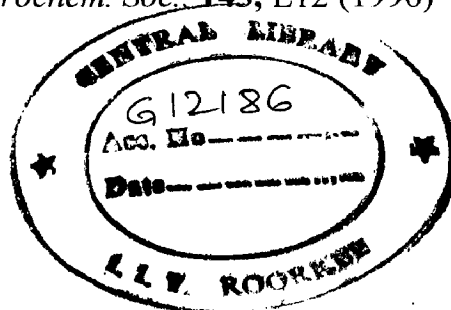
2. Here in this study, the proposed model is mainly based on the thermodynamics involved in the working of a fuel cell. Implementation of transport phenomenon in suggesting further models can provide better simulation of a liquid-feed direct methanol fuel cell.
3. Here in this study, the model is proposed under ideal gas condition. A real gas assumption can provide a more tuned and complex model to obtain more accurate results.

References

1. Z. H. Wang, and C. Y. Wang, *J. of The Electrochem. Society*, **150** (4) A508-A519 (2003)
2. W. F. Lin, J. T. Wang, and R. F. Savinell, *J. Electrochem. Soc.*, **144**, 1917 (1997).
3. A. Hamnett, *Catal. Today*, **38**, 445 (1997)
4. S. C. Thomas, X. Ren, and S. Gottesfeld, *J. Electrochem. Soc.*, **146**, 4354 (1999)
5. L. Liu, C. Pu, R. Viswanathan, Q. Fan, R. Liu, and E. S. Smotkin, *Electrochem. Acta*, **43**, 3657 (1998)
6. E. Hayden, *Catal. Today*, **38**, 473 (1997)
7. T. Page, R. Johnson, J. Hormes, S. Noding, and B. Rambabu, *J. Electroanal. Chem.*, **485**, 34 (2000)
8. X. Ren, T. E. Springer, and S. Gottesfeld, *J. Electrochem. Soc.*, **147**, 92 (2000)
9. S. Arico, P. Creti, E. Modica, G. Monforte, V. Baglio, and V. Antonucci, *Electrochem. Acta*, **45**, 4319 (2000)
10. M. K. Ravikumar and A. K. Shukla, *J. Electrochem. Soc.*, **143**, 2601 (1996)
11. S. R. Narayanan, H. Frank, B. Jeffries-Nakamura, M. Smart, W. Chun, G. Halpert, J. Kosek, and C. Cropley, in *Proton Conducting Membrane Fuel Cells I*, S. Gottesfeld, G. Halpert, and A. Landgrebe, Editors, PV 95-23, p. 278, The Electrochemical Society Proceedings Series, Pennington, NJ (1995)
12. X. Ren, T. A. Zawodzinski, Jr., F. Uribe, H. Dai, and S. Gottesfeld, in *Proton Conducting Membrane Fuel Cells I*, S. Gottesfeld, G. Halpert, and A. Landgrebe, Editors, PV 95-23, p. 284, The Electrochemical Society Proceedings Series, Pen-

nington, NJ (1995)

13. X. Ren, T. E. Springer, T. A. Zawodzinski, and S. Gottesfeld, *J. Electrochem. Soc.*, **147**, 466 (2000)
14. V. Tricoli, N. Carretta, and M. Bartolozzi, *J. Electrochem. Soc.*, **147**, 1286 (2000)
15. T. I. Valdez and S. R. Narayanan, in *Proton Conducting Membrane Fuel Cells I*, S. Gottesfeld, T. F. Fuller, and G. Halpert, Editors, PV 98-27, p. 380, The Electrochemical Society Proceedings Series, Pennington, NJ (1998)
16. S. Hikita, K. Yamane, and Y. Nakajima *JSAE Rev.*, **22**, 151 (2000)
17. J. T. Wang, S. Wasmus, and R. F. Savinell, *J. Electrochem. Soc.*, **143**, 1233 (1996)
18. P. S. Kauranen and E. Skou, *J. Electroanal. Chem.*, **408**, 189 (1996)
19. G. Halpert, S. R. Narayanan, T. Valdez, W. Chun, H. Frank, A. Kindler, S. Surampudi, J. Kosek, C. Cropley, and A. LaConti, in *Proceedings of the 32nd Intersociety Energy Conversion Engineering Conference*, Vol. 2, p. 774, AIChE, New York (1997)
20. M. Baldauf and W. Preidel, *J. Power Sources*, **84**, 161 (1999)
21. X. Ren, P. Zelenay, S. Thomas, J. Davey, and S. Gottesfeld, *J. Power Sources*, **86**, 111 (2000)
22. M. Mench, S. Boslet, S. Thynell, J. Scott, and C. Y. Wang, in *Direct Methanol Fuel Cells*, The Electrochemical Society Proceedings Series, Pennington, NJ (2001) S. R. Narayanan, S. Gottesfeld, and T. Zawodzinski, Editors, PV 2001 4, p. 241, The Electrochemical Society Proceedings Series, Pennington, NJ (2001)
23. M. Mench and C. Y. Wang, *J. Electrochem. Soc.*, **150**, A79 (2003)
24. X. Ren, M. S. Wilson, and S. Gottesfeld, *J. Electrochem. Soc.*, **143**, L12 (1996)



25. S. Gottesfeld and M. S. Wilson, in *Energy Storage Systems for Electronics Devices*, T. Osaka and M. Datta, Editors, p. 487, Gordon and Breach Science Publishers, Singapore (2000)
26. S. F. Baxter, V. S. Battaglia, and R. E. White, *J. Electrochem. Soc.*, **146**, 437 (2000)
27. J.-T. Wang and R. F. Savinell, in *Electrode Materials and Processes for Energy Conversion and Storage*, S. Srinivasan, D. D. Macdonald, and A. C. Khandkar, Editors, PV 94-23, p. 326, The Electrochemical Society Proceedings Series, Pennington, NJ (1994)
28. A. Kulikovskiy, J. Divisek, and A. A. Kornyshev, *J. Electrochem. Soc.*, **147**, 953 (2000)
29. A. A. Kulikovskiy, *J. Appl. Electrochem.*, **30**, 1005 (2000)
30. H. Dohle, J. Divisek, and R. Jung, *J. Power Sources*, **86**, 469 (2000)
31. K. Scott, P. Argyropoulos, and K. Sundmacher, *J. Electroanal. Chem.*, **477**, 97 (1999)
32. K. Sundmacher and K. Scott, *Chem. Eng. Sci.*, **54**, 2927 (1999)
33. P. Argyropoulos, K. Scott, and W. M. Taama, *J. Appl. Electrochem.*, **30**, 899 (2000)
34. K. Sundmacher, T. Schultz, S. Zhou, K. Scott, M. Ginkel, and E. D. Gilles, *Chem. Eng. Sci.*, **56**, 333 (2001)
35. Z. H. Wang, C. Y. Wang, and K. S. Chen, *J. Power Sources*, **94**, 40 (2001)
36. C. Y. Wang and P. Cheng, *Adv. Heat Transfer*, **30**, 93 (1997)
37. P. Argyropoulos, K. Scott, and W. M. Taama, *Chem. Eng. J.*, **78**, 29 (2000)
38. T. Wilmarth and M. Ishii, *Int. J. Heat Mass Transf.*, **37**, 1749 (1994)
39. G. Wolk, M. Dreyer, and H. J. Rath, *Int. J. Multiphase Flow*, **26**, 1037 (2000)
40. K. A. Triplett, S. M. Ghiaasiaan, S. I. Abdel-Khalik, A. LeMouel, and B. N. Mc-

Cord, *Int. J. Multiphase Flow*, **25**, 395 (1999)

41. T. Fukano and A. Kariyasaki, *Nucl. Eng. Des.*, **141**, 59 (1993)
42. S. Irandous and B. Anderson, *Comput. Chem. Eng.*, **13**, 519 (1989)
43. E. L. Cussler, *Difusion: Mass Transfer in Fluid Systems*, Cambridge University Press, New York (1984)
44. C. L. Yaws, *Handbook of Transport Property Data: Viscosity, Thermal Conductivity, and Diffusion Coefficients of Liquids and Gases*, Gulf Pub Co, Houston, TX (1995)
45. M. L. McGlashan and A. G. Williamson, *J. Chem. Eng. Data*, **21**, 196 (1976)
46. F. D. Incropera and D. P. DeWitt, *Fundamentals of Heat and Mass Transfer*, John Wiley & Sons, Inc., New York (1985)
47. S. Gottesfeld and T. A. Zawodzinski, *Adv. Electrochem. Sci. Eng.*, **6**, 195 (1997)
48. A. Parthasarathy, S. Srinivasan, A. J. Appleby, and C. R. Martin, *J. Electrochem. Soc.*, **139**, 2530 (1992)
49. G. Lu and C. Y. Wang, Electrochemical Engine Center (ECEC! Technical Report No. 2002-04 The Pennsylvania State University, University Park, PA (2002)
50. C. Lim and C. Y. Wang, *J. Power Sources*, **13**, 145 (2003)
51. Milo D. Koretsky, *Engineering and Chemical Thermodynamics*, John Wiley & sons, Inc., NJ (2004)
52. Y.V.C. Rao, *Chemical Engineering Thermodynamics*, Universities Press (India) Limited, A.P. (1997)
53. J.M. Smith, H.C. Van Ness, and M.M. Abbott, *Chemical Engineering Thermodynamics*, Tata McGraw-Hill, NY. (2003)

Annexure - A

Table A.1:

Formula	Name	Phase	$\Delta G_{rxn,298}^0$ (kJ/mole)
CH ₃ OH	Methanol	L	-166.34
CO ₂	Carbon dioxide	G	-394.36
H ₂ O	Water	L	-237.14
O ₂	Oxygen	G	0 (as free element in nature)

Table A.2:

Formula	Name	Phase	$\Delta H_{rxn,298}^0$ (kJ/mole)
CH ₃ OH	Methanol	L	-238.73
CO ₂	Carbon dioxide	G	-393.51
H ₂ O	Water	L	-285.83
O ₂	Oxygen	G	0 (as free element in nature)

Table A.3:

Formula	Name	A	B x 10 ⁻³	C x 10 ⁻⁶	D x 10 ⁻⁵	E x 10 ⁹
CH ₃ OH	Methanol	2.211	12.216	-3.45		
CO ₂	Carbon dioxide	5.457	1.045		-1.157	
H ₂ O	Water	3.470	1.45		0.121	
O ₂	Oxygen	3.639	0.506		-0.227	

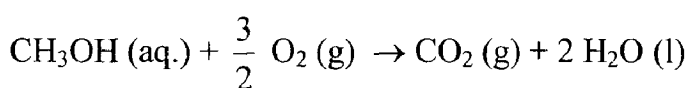
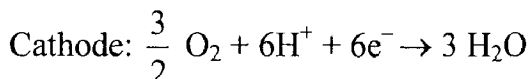
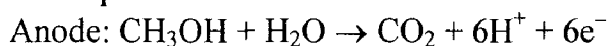
Annexure - B

Sample Calculations:

Case – 1 ($T = 80^{\circ}\text{C}$, $P = 1 \text{ atm}$)

Step-1 & 2:

Cell equation:



Here, $n_e = 6$

Step-3 & 4:

At, $T = 80^{\circ}\text{C}$, $P = 1 \text{ atm}$ & $\varepsilon = 0.99$ (assumed)

$$p_{\text{CO}_2} = P \cdot \frac{\varepsilon}{0.5(\varepsilon + 5)},$$

$$p_{\text{H}_2\text{O}} = P \cdot \frac{2\varepsilon}{0.5(\varepsilon + 5)},$$

$$p_{\text{CH}_3\text{OH}} = P \cdot \frac{(1 - \varepsilon)\varepsilon}{0.5(\varepsilon + 5)}, \text{ and}$$

$$p_{\text{O}_2} = P \cdot \frac{\frac{3}{2}(1 - \varepsilon)}{0.5(\varepsilon + 5)}$$

$$K = \frac{[p_{\text{CO}_2}] \times [p_{\text{H}_2\text{O}}]^2}{[p_{\text{CH}_3\text{OH}}] \times [p_{\text{O}_2}]^{\frac{3}{2}}} \cdot K_{\phi} P^{(v_i)}$$

At, $P = 1 \text{ atm}$, $K_{\phi} = 1$

Substituting the values, we get

$$K = 1.22 \times 10^{-5}$$

Step-5:

$$\Delta G_{rxn,298}^0 = \{\Delta G_{rxn,298}^0 [\text{CO}_2] + 2 \Delta G_{rxn,298}^0 [\text{H}_2\text{O}]\} - \{\Delta G_{rxn,298}^0 [\text{CH}_3\text{OH}] + \frac{3}{2} \Delta G_{rxn,298}^0 [\text{O}_2]\}$$

Taking values of Gibbs free energy of formation at 298 K and 1 bar from Annexure-A, Table A.1

$$\begin{aligned} \Delta G_{rxn,298}^0 &= \{(-394.36) + 2 (-237.14)\} - \{(-166.34) + \frac{3}{2} (0)\} \\ &= -702.3 \text{ kJ} \end{aligned}$$

$$\begin{aligned} \Delta G_{rxn,T} &= \Delta G_{rxn,298}^0 + RT \ln[K] \\ &= -702300 + 8.314 \times 353 \times \ln(1.22 \times 10^{-5}) \\ &= -735.505 \text{ kJ} \end{aligned}$$

Step-6:

$$\begin{aligned} \Delta H_{rxn,298}^0 &= \{\Delta H_{rxn,298}^0 [\text{CO}_2] + 2 \Delta H_{rxn,298}^0 [\text{H}_2\text{O}]\} - \{\Delta H_{rxn,298}^0 [\text{CH}_3\text{OH}] + \\ &\frac{3}{2} \Delta H_{rxn,298}^0 [\text{O}_2]\} \end{aligned}$$

Taking values of enthalpy of formation at 298 K and 1 bar from Annexure-A, Table A.2

$$\begin{aligned} \Delta H_{rxn,298}^0 &= \{(-393.51) + 2 (-285.83)\} - \{(-238.73) + \frac{3}{2} (0)\} \\ &= -726.44 \text{ kJ} \end{aligned}$$

$$\begin{aligned} \Delta H_{rxn,T} &= \Delta H_{rxn,298}^0 + R \left[\Delta A (T-298) + \frac{\Delta B}{2} (T^2-298^2) + \frac{\Delta C}{3} (T^3-298^3) \right. \\ &\quad \left. - \frac{\Delta D}{1} \left(\frac{1}{T} - \frac{1}{298} \right) + \frac{\Delta E}{4} (T^4-298^4) \right] \end{aligned}$$

Taking values of A, B, C, D and E from Annexure-A, Table A.3

$$\begin{aligned} \Delta A &= \{5.457 + 2 \times 3.470\} - \{2.211 + \frac{3}{2} \times 3.639\} \\ &= 4.7275 \end{aligned}$$

Similarly, $\Delta B = -9.03 \times 10^{-3}$

$\Delta C = 3.45 \times 10^{-6}$

$\Delta D = -0.688 \times 10^5$

$\Delta E = 0$

$$\Delta H_{rxn,T} = -726440 + 8.314 [4.7275 (353-298) + \frac{-9.03 \times 10^{-3}}{2} (353^2-298^2) + \frac{3.45 \times 10^{-6}}{3} (353^3-298^3) - \frac{-0.688 \times 10^5}{1} (\frac{1}{353} - \frac{1}{298}) + \frac{0}{4} (353^4-298^4)]$$

Thus,

$\Delta H_{rxn,T} = -725.455 \text{ kJ}$

Step-7:

$$E^0 = - \frac{\Delta G_{rxn,298}^0}{n_e F}$$

$$= - \frac{-702300}{6 \times 96485}$$

$$= 1.213 \text{ V}$$

$$E_{Nernst} = E^0 - \frac{2.303 RT}{n_e F} \log Q$$

Where, $Q = K_{P=1 \text{ atm}}$

Thus, $Q = 1.22 \times 10^{-5}$

Therefore,

$$E_{Nernst} = 1.213 - \frac{2.303 \times 8.314 \times 353}{6 \times 96485} \log (1.22 \times 10^{-5})$$

$$= 1.270 \text{ V}$$

Step-8:

Since,

$W_{cell} = - \Delta G_{rxn,T}$

$\Rightarrow W_{cell} = - (-735.505 \text{ kJ})$

$= 735.505 \text{ kJ}$

Step-9:

Since,

$$Q_P = H_P - H_R$$

$$\Rightarrow Q_P = 1452.880 \text{ kJ}$$

Step-10:

$$\eta_{th} = \frac{W_{cell}}{Q_P}$$

$$\Rightarrow \eta_{th} = \frac{735.505}{1452.880}$$

$$= 0.506$$

$$= 50.6 \%$$

Step – 11:

At $n_c = 2.33 \times 10^{-6} \text{ gm-mole/sec}$

$$I = n_c n_e F$$

$$= 2.33 \times 10^{-6} \times 6 \times 96485$$

$$= 1.35 \text{ A}$$

At, $A = 5 \text{ cm}^2$

$$I_{density} = I / A$$

$$= 1.35 / 5$$

$$= 0.27 \text{ A/cm}^2$$

Step – 12:

At, $ASR_{cell} = 4.737 \text{ } \Omega - \text{cm}^2$

$$V_{cell} = E_{Nernst} - I_{density} \times ASR_{cell}$$

$$= 1.270 - 0.27 \times 4.737$$

$$= 0.1 \text{ V}$$

Annexure - C

Table C.1:

<i>Temperature, K</i>	$\Delta G_{rxn,T}$ (kJ) <i>(P = 1 bar)</i>	$\Delta G_{rxn,T}$ (kJ) <i>(P = 2 bar)</i>	$\Delta G_{rxn,T}$ (kJ) <i>(P = 3 bar)</i>	$\Delta G_{rxn,T}$ (kJ) <i>(P = 4 bar)</i>	$\Delta G_{rxn,T}$ (kJ) <i>(P = 5 bar)</i>
308	-731.272	-730.378	-729.869	-729.497	-729.210
318	-732.213	-731.289	-730.764	-730.38	-730.083
333	-733.624	-732.657	-732.107	-731.705	-731.394
348	-735.035	-734.024	-733.45	-733.029	-732.704
353	-735.505	-734.48	-733.897	-733.471	-733.141

Table C.2:

<i>Temperature, K</i>	$\Delta H_{rxn,T}$ (kJ) <i>(P = 1 bar)</i>
308	-726.248
318	-726.062
333	-725.793
348	-725.538
353	-725.455

Table C.3:

<i>Temperature, K</i>	W_{net} (kJ) <i>(P = 1 bar)</i>	W_{net} (kJ) <i>(P = 2 bar)</i>	W_{net} (kJ) <i>(P = 3 bar)</i>	W_{net} (kJ) <i>(P = 4 bar)</i>	W_{net} (kJ) <i>(P = 5 bar)</i>
308	731.272	730.378	729.869	729.497	729.210
318	732.213	731.289	730.764	730.38	730.083
333	733.624	732.657	732.107	731.705	731.394
348	735.035	734.024	733.45	733.029	732.704
353	735.505	734.48	733.897	733.471	733.141

Table C.4:

<i>Temperature (K)</i>	<i>Thermal Efficiency (η_{th}, %)</i> <i>(P = 1 bar)</i>
308	50.3
318	50.4
333	50.5
348	50.6
353	50.7

Table C.5:

Temperature (K)	Nernst Potential (E_{Nernst}, V) <i>($P = 1 \text{ bar}$)</i>
308	1.264
318	1.265
333	1.267
348	1.269
353	1.27

Table C.6:

Fuel Flow Rate (n_c, gm-mole/sec)	Cell Current (I, A)
2.33×10^{-6}	1.35
2.16×10^{-6}	1.25
1.51×10^{-6}	0.875
4.3×10^{-7}	0.25
2.15×10^{-7}	0.125

Table C.7:

Cell Current (I, A)	Cell Active Area, cm²	Current Density, A/ cm²
1.35	5	0.27
1.25	5	0.25
0.875	5	0.175
0.25	5	0.05
0.125	5	0.025

Table C.8:

Current Density, A/ cm²	Cell Voltage (V)
0.27	0.1
0.25	0.2
0.175	0.4
0.05	0.6
0.025	0.7

Nomenclature

1. Notations (Engineering Thermodynamics)

d	Exact differential	
\bar{h}	Molar enthalpy	[kJ/kmol]
\bar{g}	Molar Gibbs function (or energy)	[kJ/kmol]
\bar{s}	Molar entropy	[kJ/kmol/K]
E	Total energy	[kJ/kmol]
H	Enthalpy	[kJ/kmol]
I	Irreversibility	[kJ/kmol]
KE	Kinetic energy	[kJ/kmol]
N	Number of moles	
P	Pressure	[Pa]
PE	Potential energy	[kJ/kmol]
Q	Heat energy	[kJ/kmol]
S	Entropy	[kJ/K]
T	Absolute temperature	[K]
T_c	Constant temperature	[K]
U	Internal energy	[kJ/kmol]
V	Volume	[m ³]
W	Work energy	[kJ/kmol]
X	Energy	[kJ/kmol]

Greek

δ	Inexact differential
η_{th}	Thermal efficiency
η_{2nd}	Second Law efficiency
Δ	Products minus reactants

Subscripts

1, 2, 3, 4	States 1, 2, 3, 4
adiabatic	Adiabatic (entropy)
Carnot	Carnot cycle
f	Formation (enthalpy, Gibbs function)
gen	Generated (entropy)
H	High (temperature)
in	Input (heat)
L	Low temperature
net	Net (work)
out	Output (heat)
P	Products
R	Reactants
rev	Reversible (heat, work)

surr	Surroundings (entropy)
sys	System (entropy)
th	Thermal (efficiency)
total	Total (entropy)

Superscript

o	Standard reference state (25°C and 1 atm)
---	---

2. Notations (Chemical Thermodynamics)

d	Exact differential	
E	Voltage difference across the electrodes, E° standard potential	[V]
F	Faraday's constant, charge carried by a mole of electrons (96,485 C/mol)	
G	Gibbs energy	[kJ/kmol]
H	Enthalpy	[kJ/kmol]
K_{eq}	Reaction quotient at equilibrium conditions	
n	Number of moles	
n_e	Number of electrical charges	
P	Pressure	[Pa]
P°	Standard reference pressure (1 atm)	
Q	General reaction quotient	
Q	Heat energy	[kJ/kmol]
R	Molar gas constant (8.3145 kJ/mol/K)	
S	Entropy	[kJ/K]
T	Absolute temperature	[K]
U	Internal energy	[kJ/kmol]
V	Volume	[m ³]
W	Work energy	[kJ/kmol]
W_e	Electrochemical work, $W_{e,\text{max}}$ maximum electrochemical work	[kJ/mol]

Greek

δ	Inexact differential
Δ	Products minus reactants
∂	Partial derivative

Subscripts

1, 2	States 1, 2
T, P	Constant temperature and pressure
rev, irrev	Reversible and irreversible process
A, B, M, N	Reactant gases
i	Component i

Superscripts

$^\circ$	Standard reference state (Gibbs energy)
a, b, m, n	Stoichiometric coefficients

3. Notations (Electrochemical Kinetics)

$\Delta \bar{G}^{\ddagger}$	Gibbs energy of activation, $\Delta \bar{G}_c^{\ddagger}$ Gibbs chemical energy of activation, $\Delta \bar{G}_{chem}^{\ddagger}$ Gibbs chemical energy of activation	[kJ/mol]
[]	Concentration, [] _s surface concentration	[Molarity] or [mol/cm ³]
A	Active area of the electrode	[cm ²]
e^-	Electron	
F	Faraday's constant (96,485 C/mol)	
h	Planck's constant (6.6261×10^{-34} J · s)	
H^+	Proton	
i	Current density	[A/cm ²]
I	Current	[A]
i_0	Exchange current density	[A/cm ²]
j	Flux of reactant reaching the surface	[mol/sec]
k	Rate coefficient, k_0 in derivation of the Butler-Volmer equation, k_f forward rate coefficient, k_b backward rate coefficient	[1/s]
k_B	Boltzmann's constant	
n	Number of moles	
Ox	Species that is the product of an oxidation reaction	
R	Molar gas constant (8.3145 kJ/mol/K)	
Red	Species that is the product of a reduction reaction	
T	Absolute temperature	[K]
W_e	Electrical work	[kJ]

Greek

β	Transfer coefficient	
ϕ	Potential	[V]
η	Overpotential (or polarization)	[V] or [mV]

Subscripts

b	Backward (rate coefficient, flux)
c	Chemical (Gibbs energy)
f	Forward (rate coefficient, flux)
rev	Reversible (potential)